TAMPEREEN TEKNILLINEN YLIOPISTO
TAMPERE UNIVERSITY OF TECHNOLOGY

Kirsi Saarinen

Utilising Shear Stress Modelling in Reliability Studies of Polymeric Interconnections in Electronics

Julkaisu 1019 • Publication 1019

Tampere 2012

Tampereen teknillinen yliopisto. Julkaisu 1019
Tampere University of Technology. Publication 1019

Kirsi Saarinen

Utilising Shear Stress Modelling in Reliability Studies of Polymeric Interconnections in Electronics

Thesis for the degree of Doctor of Science in Technology to be presented with due permission for public examination and criticism in Tietotalo Building, Auditorium TB109, at Tampere University of Technology, on the 24th of February 2012, at 12 noon.

Tampereen teknillinen yliopisto - Tampere University of Technology
Tampere 2012

ISBN 978-952-15-2759-3 (printed)
ISBN 978-952-15-2774-6 (PDF)
ISSN 1459-2045

ABSTRACT

Polymeric interconnections in electronics are used in various applications and consequently, they may be exposed to various environments during their life-time. Accelerated life tests are typically used to study their reliability in different environments. However, the tests are fairly time-consuming and often expensive. If modelling with accurate results could be utilised when studying reliability, time and cost savings could be achieved as the need for actual testing would decrease. In this study possibilities to utilise shear stress modelling in the prediction of polymeric interconnection reliability under humid and thermal environments were investigated.

It was observed that if the failure mechanism of the polymeric interconnections is related to shear stresses, shear stress modelling can be utilised in reliability studies in thermal environments. For example, delamination may be one manifestation of failure mechanisms related to shear stress. If the materials or dimensions of polymeric interconnections are changed so that failure mechanisms will not change, shear stress modelling together with the reliability data of the initial structure can be used to estimate failure times and places of the new structure. On the other hand, if the failure mechanism of the polymeric interconnection is related to thermal expansion of the adhesive matrix, strain modelling which calculates the changes in thickness of an adhesive layer between contacts seems feasible in reliability studies. In addition it was observed in this study that reliability prediction of polymeric interconnections in humid environments is extremely difficult due to the numerous factors causing failures in humid environments. It was not possible to use shear stress modelling alone, as the factors causing failure are not only related to shear stresses. However, if shear stress modelling together with adhesion measurements is used, estimation of failure times in a constant humidity test seems to be possible.

ACKNOWLEDGEMENTS

This work was carried out at the Department of Electronics of the Faculty of Computing and Electrical Engineering at Tampere University of Technology (TUT) during the period 2008-2012.

This work was supported financially by the TUT President's Doctoral Programme, the Finnish Cultural Foundation, the KAUTE Foundation, the HPY Research Foundation, the EIS Foundation, the Tuula and Yrjö Neuvo Fund and the Ulla Tuominen Foundation, whose support is here gratefully acknowledged.

I want to thank my supervisor Professor Lauri Kettunen for his guidance and support for finalizing this thesis. I am most grateful to my supervisor Laura Frisk, D.Sc., whose guidance, encouragement and support were essential for the completion of this thesis. I also want to express my gratitude to my former supervisor, Adjunct Professor Pekka Heino for the guidance and support at the beginning of this study. In addition, I want to thank my co-authors Adjunct Professor Leena Ukkonen and Anne Cumini, D.Sc. Furthermore, I am thankful to the pre-examiners Professor Christopher Bailey and Helge Kristiansen, D.Sc. for their valuable comments and suggestions.

I am very grateful to my colleagues in the Packaging and Reliability Group for the help and support during this process. Especially, I want to thank Janne Kiilunen, M.Sc. for his help in arranging the experiments, and Kati Kokko, D.Sc., Janne Kiilunen, M.Sc., Anniina Parviainen M.Sc. and Sanna Lahokallio M.Sc. for the encouragement and fruitful discussions. I am also very grateful to the personnel in the Radio Frequency Identification Group for helping me with the measurements of radio frequency identification tags. Additionally, I want to thank Marko Silvennoinen, M.Sc. at Optoelectronics Research Centre for his help with the adhesion tests.

Most of all, I am very grateful to Kimmo and my family for their loving support and encouragement.

Tampere, January 2012

Kirsi Saarinen

Supervisors	Professor Lauri Kettunen Department of Electronics Tampere University of Technology Finland
	D.Sc. Laura Frisk Department of Electronics Tampere University of Technology Finland
	Adjunct Professor Pekka Heino Department of Electronics Tampere University of Technology Finland
Pre-examiners	Professor Christopher Bailey Computational Mechanics and Reliability School of Computing and Mathematical Sciences University of Greenwich United Kingdom
	D.Sc. Helge Kristiansen Conpart AS Norway
Opponent	Adjunct Professor Olli Salmela Nokia Siemens Networks Finland

TABLE OF CONTENTS

LIST OF PUBLICATIONS

This thesis consists of an extended summary and the following publications:

I. Frisk, L., Saarinen, K. and Cumini, A. “Reliability of ACF interconnections on FR-4 substrates”, IEEE Transactions on Components and Packaging Technologies, Vol. 32, No. 4, 2010, pp. 138-147.

II. Saarinen, K. and Frisk, L. “The Effects of Temperature Profile of Accelerated Temperature Cycling Tests on the Reliability of ACA Joints in RFID Tags”, IMAPS Journal of Microelectronics and Electronic Packaging, Vol. 8, No. 1, 2011, pp. 10-15.

III. Saarinen, K., Frisk, L. and Ukkonen, L. “Effects of cycling humidity on the performance of RFID tags with ACA joints” Accepted for publication in IEEE Transactions on Reliability.

IV. Saarinen, K. and Heino, P. “Moisture Effects on Adhesion of Non-Conductive Adhesive Attachments”, Soldering & Surface Mount Technology, Vol. 22, No. 1, 2010, pp. 41-46.

V. Saarinen, K. and Frisk, L. “Changes in Adhesion of Non-Conductive Adhesive Attachments during Humidity Test”, IEEE Transactions on Components, Packaging and Manufacturing Technology, Vol. 1, No. 7, 2011, pp. 1082-1088.

VI. Saarinen, K. and Frisk, L. “Shear stress modelling of ACA joints during temperature cycling testing”, Report, Tampere University of Technology, Department of Electronics, 2011.

AUTHOR'S CONTRIBUTION

Publication I, "Reliability of ACF interconnections on FR-4 substrates", was accomplished by the present author together with the co-authors as follows: the tests were planned, the test samples assembled, the testing carried out, and the results analysed by L. Frisk. The modelling was planned with help of L. Frisk, carried out and results analysed by the present author. In the manuscript the description of experimental testing was written by L. Frisk with the help of the co-authors and of the modelling by the present author with the help of L. Frisk.

Publication II, "The Effects of Temperature Profile of Accelerated Temperature Cycling Tests on the Reliability of ACA Joints in RFID Tags", was accomplished by the present author together with the co-author as follows: the tests were planned with the help of the co-author, the testing carried out, and the results analysed by the present author. The SEM analysis was conducted at the Department of Material Science at Tampere University of Technology under the supervision of the present author. The present author wrote the manuscript with the help of the co-author.

Publication III, "Effects of cycling humidity on the performance of RFID tags with ACA joints", accomplished by the present author together with the co-authors as follows: the tests were planned with the help of L. Frisk, the testing carried out, and the results analysed by the present author. The measurements for the radio frequency identification tags were carried out by the present author with the help of L. Ukkonen. The SEM analysis was conducted at the Department of Material Science at Tampere University of Technology under the supervision of the present author. The present author wrote the manuscript with the help of the co-authors.

Publication IV, "Moisture Effects on Adhesion of Non-Conductive Adhesive Attachments", accomplished by the present author together with the co-author as follows: the tests and the modelling were planned together with the co-author, the test samples assembled, the tests carried out, the experimental results analysed, the modelling carried out, and the modelling results analysed by the present author. The present author wrote the manuscript with the help of the co-author.

Publication V, "Changes in Adhesion of Non-Conductive Adhesive Attachments during Humidity Test", accomplished by the present author together with the co-author as follows: the tests and the modelling were planned together with the co-author, the test samples assembled, the tests carried out, the experimental results analysed, the modelling carried out, and the modelling results analysed by the present author. The SEM analysis was conducted at the Department of Material Science at Tampere University of Technology under the supervision of the present author. The present author wrote the manuscript with the help of the co-author.

Publication VI, "Shear stress modelling of ACA joints during temperature cycling testing", accomplished by the present author together with the co-author as follows: the tests were planned, the test samples assembled, and the testing carried out by the co-author. The experimental results were analysed, the modelling planned with the help of the co-author, the modelling carried out and the modelling results analysed by the present author. The SEM analysis was conducted at the Department of Material Science at Tampere University of Technology under the supervision of the co-author

and the failure analysis was carried out by the co-author. The present author wrote the manuscript with the help of the co-author.

LIST OF ABBREVIATIONS AND SYMBOLS

ACA	Anisotropic Conductive Adhesive
ACF	Anisotropic Conductive Adhesive Film
ACP	Anisotropic Conductive Adhesive Paste
Al_2O_3	Aluminium Oxide, Alumina
ALT	Accelerated Life Test
COF	Chip on Flex
COG	Chip on Glass
CSP	Chip Scale Package
CME	Coefficient of Moisture Expansion
CTE	Coefficient of Thermal Expansion
DMA	Dynamic Mechanical Analysis
FEM	Finite Element Modelling
FR-4	Grade of substrate material
ICA	Isotropic Conductive Adhesive
I/O	Input/Output
LCP	Liquid Crystal Polymer
NCA	Non-Conductive Adhesive
NCF	Non-Conductive Adhesive Film
NCP	Non-Conductive Adhesive Paste
OLED	Organic Light-Emitting Diodes
PDF	Probability Density Function
PDP	Plasma Display Panel
PET	Polyethylene Terephtalate
RCC	Resin-Coated Copper Foil
RFID	Radio Frequency Identification
RH	Relative Humidity
SEM	Scanning Electron Microscopy
SMT	Surface Mount Technology
TA	Thermal Analysis
TMA	Thermo-Mechanical Analysis
TCP	Tape Carrier Package
UHF	Ultra High Frequency
α	Coefficient of Thermal Expansion

β	Shape Parameter of Weibull Distribution or Coefficient of Moisture Expansion
γ_{xy}, γ_{yz}, γ_{xz}	Shear Strains
Δl	Change in Length
ΔT	Temperature Change
ε_0	Thermal Strain / Hygroscopic Strain
ε_h	Hygroscopic Strain
ε_x, ε_y, ε_z	Normal Strains
σ_x, σ_y, σ_z	Normal Stresses
τ_{xy}, τ_{yz}, τ_{xz}	Shear Stresses
η	Scale Parameter of Weibull Distribution
B	Element Strain-Displacement Matrix
C	Number of Censored Samples / Moisture Concentration
C_{sat}	Saturated Moisture Concentration
D	Diffusion Coefficient / Material Matrix
dl/l_0	Relative Dimensional Change
dT	Temperature Change
E	Young's Modulus
F	Number of Failed Samples
$f(t)$	Probability Density Function
l_0	Initial Length
M_t	Mass of Absorbed Moisture at Time t
M_{sat}	Saturated Mass of Absorbed Moisture
q	Displacements
t	Time
T_g	Glass Transition Temperature
V	Volume
x,y,z	Dimensions

1 Introduction

Currently the trend in electronics is towards smaller and lighter devices with better performance and larger number of input/outputs (I/Os). At the same time better reliability, environmental friendliness and lower cost are also called for. [Lin08b] [Yim03] Isotropic conductive adhesives (ICAs), anisotropic conductive adhesives (ACAs) and non-conductive adhesives (NCAs) are used to achieve these goals due to their numerous advantages compared to traditional solder joints with underfills [Li06]. These polymeric interconnections enable finer pitches, lower processing temperatures, better environmental friendliness and reduced costs [Li06][Lin08b].

Use of ACAs as a replacement of solders has gained popularity in recent years [Lin08b]. ACAs are widely used in flip chip joints of different applications, such as radio frequency identification tags (RFID tags) [Ras04][Yim06]. In addition to ACAs, NCAs are a promising alternative to solders [Kim08a]. By using NCAs instead of ACAs, even finer pitches and lower costs, as well as better electrical performance are achieved [Kim08a][Liu99]. However, limited reliability data on polymeric interconnections is one of the limitations, which has inhibited the wider use of these materials [Liu98b][Teh04][Yim03].

Polymeric interconnections are used in applications which may be exposed to various environmental conditions during their lifetime. Consequently, reliability problems may occur, if operation of the product degrades or fails [Lin08b]. Accelerated life tests (ALTs) are used to study the reliability in different environments [Jen95][Suh02]. With these tests statistical reliability data and information of typical failure modes and mechanisms are achieved significantly faster compared to testing in the products operating environment [Suh02]. Although the results are achieved significantly faster, ALTs are still fairly time-consuming and often expensive, because the test conditions and failure mechanisms need to correspond to those in the operating environment [Jen95][Suh02]. If modelling could be utilised in the prediction of reliability the results could be achieved more quickly. In addition, cost saving could be achieved when the use of models would reduce the need for testing. [Suh02]

Modelling of polymer interconnections in ALTs is challenging due to the various factors which may affect the materials and material interfaces during testing. The failure process may be chemical, physical or mechanical [Bro99][Jen95][Tum01], and in practice different factors may act simultaneously [Lai96]. Nevertheless, a good predictive reliability model should be simple, suitable for new applications or new environments and clearly indicate the causes and the effects [Suh02].

1.1 Objectives and scope of the thesis

The object of this study was to investigate whether it is possible to use relatively simple shear stress models to predict reliability in thermal and humid ALTs. The aim was to examine if the modelling together with the reliability data of a test with one type of test structure could be used in prediction of reliability of slightly changed test structure or test. The test structures were varied by changing thicknesses of test chips and substrates, or using different adhesive materials. Thermal and humidity tests with constant or fluctuating conditions were used. Tests were varied using different profiles with

different temperatures and humidity levels. In addition, the shear stress models were used together with results of adhesion strength tests to study if modelling could be utilised in prediction of failures in humid environment when the deterioration of adhesion strength is possible to estimate. The modelling was done using finite element method. The predictions made on the basis of the modelling were compared to experimental results to estimate the validity of the models.

1.2 Structure of the thesis

This thesis consists of an extended summary followed by six publications. The extended summary is divided into five chapters, which provide relevant background information of the topic and present the main results. Chapter 1 gives a general introduction to the topic. Chapter 2 introduces polymeric interconnection technology and presents the test samples used in this study. Discussion about reliability and description of the test setups and reliability results used in this study are presented in Chapter 3. Chapter 4 talks about modelling, presents the main modelling results, and compares the results of modelling to the experimental results. The final conclusions and a summary of publications are presented in Chapter 5.

2 Polymeric interconnections for electronics

Adhesive attachments are an alternative to solder joints to make electrically conductive interconnections in electronics. Adhesive attachments can be formed with isotropic conductive adhesives (ICAs), anisotropic conductive adhesives (ACAs), or with non-conductive adhesives (NCAs). [Li06][Liu99] The use of adhesive attachments, especially ACAs as a replacement of solders has increased recently due to their advantages [Lin08a][Lin08b].

ICAs and ACAs are composed of polymer matrix and conductive particles [Liu99]. Polymer matrix is an insulator which provides physical and mechanical properties, such as adhesion, mechanical strength and impact strength [Li05]. The function of the polymer matrix is to provide electrical insulation, to protect joints mechanically and to provide stable adhesion [Yim99]. Electrical connection between conductors is provided through electrically conductive particles [Li05][Lin08b]. Consequently, the electrical and mechanical properties are provided by two different components, which is different from that of solders [Li06][Lin08b]. NCAs consist solely of a polymer matrix without conductive particles [Liu99]. The electrical conduction in NCA joints is created by holding conductors physically in contact [Liu99][Teh04].

Use of ACAs has gained popularity in recent years and they are widely used in flip chip joints in various applications [Lin08b][Ras04][Yim06]. On the other hand, NCAs are a promising alternative to solders and also for ACAs due to their advantages, such as even finer pitches, lower costs, and better electrical performance [Kim08a][Liu99]. Although, ACA, NCA, and ICA are all polymeric electrically conductive adhesives and may be used in similar applications, their behaviour under environmental stresses may vary a lot. The research in this work concentrates in flip chip joints using ACAs and NCAs whose bonding process is similar. Therefore, the models developed in this work may be utilised for ACA and NCA interconnects with only minor adjustments. ICAs may also be used in flip chip application. However, due to their differences compared to ACA and NCA structures they were not studied in this work. Consequently, ICAs are introduced only briefly at the beginning of this chapter and later on ACAs and NCAs are discussed in greater detail.

2.1 Isotropic conductive adhesives

ICAs contain approximately 25-30 volume% of conductive particles, which is above a percolation threshold [Liu99][Lu08][Lu10a]. Thereby, conductive particles are in contact with each other and they form a conductive net between the conductors [Lew08] [Lu10a]. The conductive particles are distributed evenly and thus the adhesive conducts to all directions [Liu99][Lu08]. As ICAs typically conduct in all directions, they are used as solders by adding ICA only at the contact areas [Liu99]. The mechanical properties of the ICA are achieved by curing of the polymer matrix [Lic05]. In addition, underfill is generally added around the joints after bonding to improve mechanical support [Liu99]. An illustration of flip chip joints using ICA is shown in Figure 1.

ICAs have typically been used as die attach adhesives, flip chip interconnections and in surface mount technology (SMT) applications [Li06][Lu10a][Yim08]. ICAs are an environmentally friendly alternative to solders and they can be used in more sensitive and low cost applications than solders due to the lower processing temperatures [Li06]

[Liu99]. However, a major drawback of ICAs compared to solders is their significantly lower electrical conductivity [Lu08]. Other limitations for wider use are low reliability, high material costs, poor mechanical impact strength, and unstable contact resistance with non-noble metals [Lu08][Yim08].

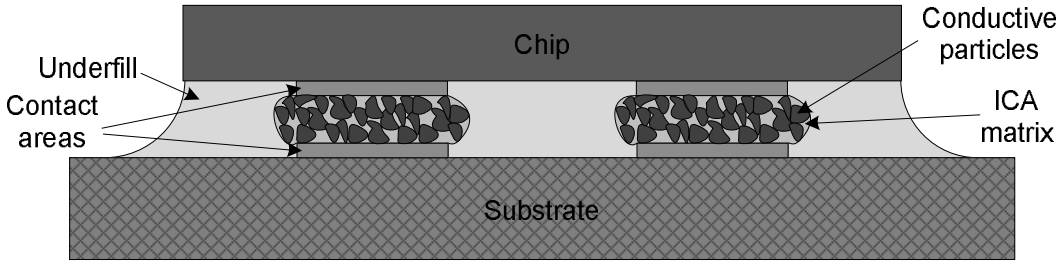

Figure 1: An illustration of flip chip joints using ICA [Li06][Yim08].

Polymer matrix in ICAs may be thermoplastic or thermosetting [Liu99]. However, most commercial ICAs are based on thermosetting polymers, such as epoxies [Li06]. Conductive particles are typically silver, gold nickel, copper or carbon particles with various shapes and sizes [Li06]. Silver flakes are generally used because of the high conductivity, maximum contact with conductors and each other and because silver oxide is electrically conductive [Li06][Lu08].

2.2 Anisotropic conductive adhesives

ACAs may be in the form of a paste (ACP) or a film (ACF) [Lin08b][Liu05]. The proportion of conductive particles in ACAs is typically between 5-10 volume%, which is below the percolation threshold [Kri98][Lew08][Lin08a][Lin08b][Liu98a]. Consequently, in ACAs the conductive particles are only in sporadic contact with each other, and ACAs serve as insulators before bonding [Kwo06a][Lin08a]. As a result, ACA can be dispensed for the whole bonding area, and no additional underfill is needed [Liu99][Liu07]. In the bonding process, contact areas, which are covered with ACA, are pressed towards each other, so that some of the conductive particles are trapped between them. The trapped particles form electrically conductive paths between the bumps on chip and the pads on substrate. Consequently, after bonding ACA conducts to z-direction, but serves still as an insulator to the other directions. [Lin08a][Lin08b] Moreover, to hold the particles in their positions and to give mechanical support, the polymer matrix is cured under pressure in the bonding process [Kri98][Kwo06a] [Liu99]. An illustration of flip chip joints using ACA is shown in Figure 2.

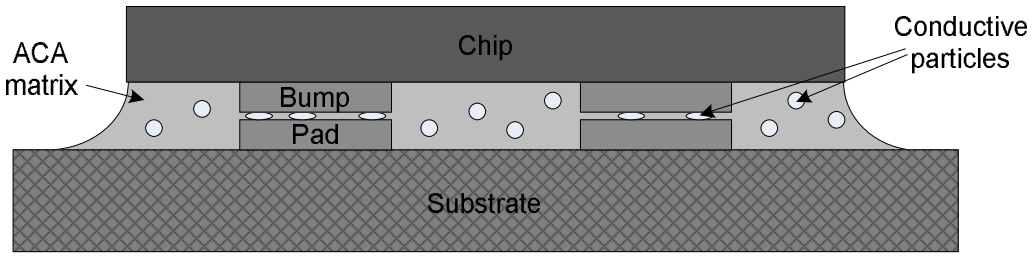

Figure 2: An illustration of flip chip joints using ACA [Li06][Lin08a].

2.3 Non-conductive adhesives

NCAs may also be in the form of paste (NCP) or film (NCF) [Cae04][Hwa09]. Electrical connection in NCA joints is achieved through mechanical contacts between bumps and pads [Liu99]. NCA left around the joints is cured to hold the contact areas in contact and to give mechanical support [Kri98][Liu99]. The bonding process of NCAs is similar to the bonding process of ACAs. NCA is also dispersed for the whole bonding area and the contact areas are pressed against each other so that NCA flows away from contacts [Liu99]. Because of the roughness of the contact surfaces, only small contact spots are formed in the joints when a low bonding pressure is used [Liu99][Yim08]. With a higher bonding pressure the number of the spots and the contact area increases by increasing the conductivity of the joints [Liu99][Yim08][Yu04]. Moreover, to increase the contact area further, stud bumps are often used in NCA attachments. These are ball joints used in wire bonding, but the wire has been cut right after the joint. Consequently, in stud bumps there is a tail which adds significant height to the bump, causing easier flow of adhesive and providing good metal-to-metal contact under pressure. [Yim03] An illustration of flip chip joints using NCA is shown in Figure 3.

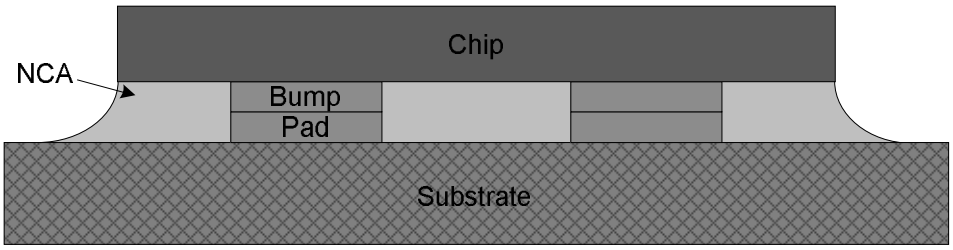

Figure 3: An illustration of flip chip joints using NCA [Li06][Yim08].

2.4 Bonding process of ACAs and NCAs

The bonding processes of NCA and ACA attachments are similar and they have the same bonding steps [Hwa09]. The process steps of ACA are shown in Figure 4. First adhesive is dispersed on the whole bonding area of a substrate [Liu07]. Pastes can be printed with screen or stencil, or dispensed with syringe dispenser [Liu07][Lyo03]. Film type adhesive is cut to a piece which covers the bonding area and is then set on the substrate by hand or pick-and-place equipment [Lyo03]. After that the film is attached on substrate by pre-bonding [Kok10][Lin06a]. In the pre-bonding adhesive film is pressed and heated with light pressure and temperature for a short time [Lin06a] [Yim98].

The next step is alignment which is illustrated in Figure 4b. The bumps on the chip are aligned with the pads on the substrate [Lin08a]. After that, pressure is applied on the back side of the chip and the chip is pressed against the substrate [Liu07]. With NCA the polymer matrix is squeezed out from the joints so that the bumps get into contact with the pads [Liu99]. With ACA some of the conductive particles are trapped between the bumps and the pads while polymer matrix is squeezed out of the joints [Lin06b] [Lin08b][Liu07]. This can be seen in Figure 4c.

When high enough pressure is applied to ACA joints, soft conductive particles, such as metal coated polymer particles, deform [Lai96]. Deformed particles have larger conduction area and better reliability [Lai96][Liu07]. On the other hand if the particles

are hard, such as nickel particles, but the bumps or pads are soft, such as gold or copper, the particles penetrate inside the soft metal [Yim98]. Thereby the conduction area also increases, and a possible insulating metal oxide layer on top of the bump or pad will be penetrated [Cha00][Liu07].

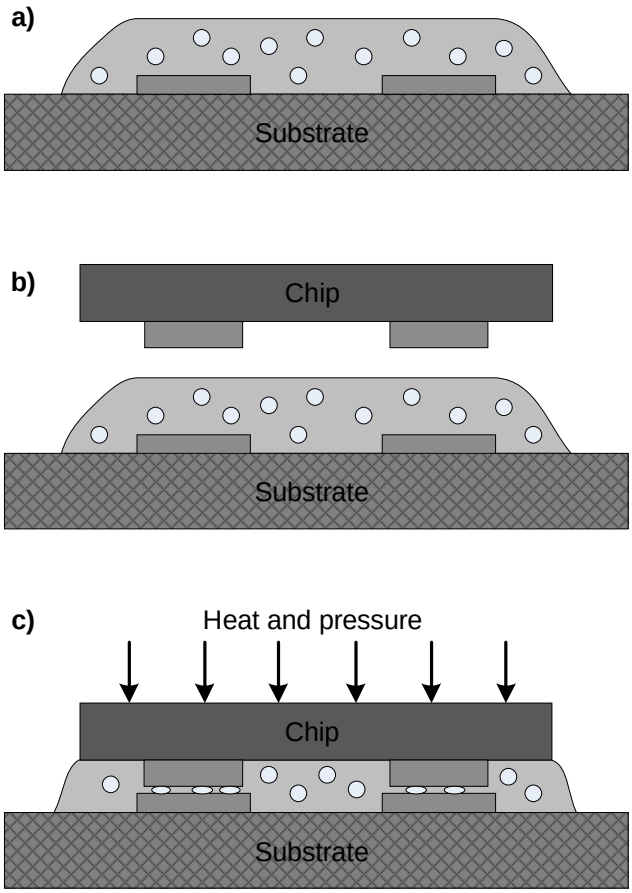

Figure 4: Steps of bonding process of ACA.

After the electrical conductivity has been ensured by the mechanical contacts of the bumps and pads to each other or to conductive particles, the polymer matrix is cured under pressure [Liu07]. During curing the polymer is hardened when the energy supplied to the polymer initiates chemical reactions [Lin08b]. Heat, UV light and added catalyst are generally used curing techniques [Lin08b][Liu07]. Heat is the most typically used one and it was used also in this study [Lin08b]. The heat was supplied though the chip and substrate. During curing the polymer matrix shrinks and forms compressive forces to the joints [Kwo04b]. These forces exert a continuous contact pressure which ensures the physical and electrical contact in the joints after the bonding [Liu07][Teh04].

2.4.1 Bonding parameters

Bonding parameters have a significant effect on the quality, performance and reliability of the joints [Lai96][Lin08b][Liu07]. The three most important bonding parameters are temperature, time and pressure [Lin08b][Sep04]. Bonding temperature and time determines the curing degree of the adhesive, which has been observed to have a significant effect on electrical conductivity, adhesion and reliability of the joints [Liu07] [Riz05][Udd04].

In under-cured joints contact resistance is higher, adhesion is lower and reliability in humid environments is weaker [Che06][Liu07][Wan08]. On the other hand, if the adhesive is heated continually beyond its fully cured state or if excessive temperature is used, the properties will deteriorate again [Liu99][Wan08]. The adhesive may decompose and turn brittle [Liu99]. In addition, resistance may increase, adhesion and impact strength may decrease, and reliability may weaken [Lin08b][Udd04][Wan08]. Greater curing degree is achieved either with longer bonding time or with higher bonding temperature. However, longer curing time increases the process time and thus decreases productivity. On the other hand, if higher bonding temperature is used, it is possible that the polymer matrix has not enough time to flow, and the conductive particles have not enough time to compress between bumps and pads and deform properly before the polymer matrix starts to solidify. [Liu07][Rau06] In addition, at high temperatures cracks and voids may be formed to the adhesive material weakening the dielectric properties [Lin08b]. Moreover, a high temperature may be harmful in sensitive applications [Liu98a].

In ACA joints high enough pressure is required to deform particles and thereby ensure a proper electrical contact [Lai96][Liu07]. In NCA joints the pressure is also critical to ensure a stable electrical contact between bumps and pads [Hwa09]. However, high pressure may impair long-term reliability of the joints [Sep04]. Under too high pressure internal elastic stress is built up in the adhesive. On the other hand, elastic deformation of metals is relatively small and under high pressure this may lead to plastic deformation. Under use or test conditions, such as high humidity and temperature, the elastic stress of the adhesive may be released, and as a result gaps in the joints may be formed, which increases contact resistance. As the deformation caused by high pressure in metals is plastic, they are unable to compensate changes in polymer parts and this may also cause formation of gaps. [Li06][Yim99] In addition, if excessive pressure is applied to metal coated polymer particles of ACAs, the metal coating may peel off and the reliability is impaired [Yim99].

In addition to the magnitude of the bonding pressure, its distribution should be even to ensure equal conductivity and reliability of all joints [Lai96][Liu07]. Therefore, besides planarity of a bonding tool, planarity of a substrate, equal heights of bumps and homogeneity of particle sizes are desirable [Lai96][Sep04]. In FR-4 substrates pad are inclined to penetrate inside the epoxy. Glass fibre hinders the penetration and therefore a distance of a glass fibre to a pad has a significant effect on the pressure distribution and reliability. [Sep04]

2.5 Materials of ACAs and NCAs

Both thermoplastic and thermosetting materials are used as polymer matrix of adhesives [Li06][Liu99]. The most significant advantage of thermoplastics is repairability of the joints, which is very difficult with thermosets [Lic05][Lin08b]. However, thermosetting materials are still the most commonly used ones because of their better strength, more robust bonds, chemical and corrosion resistance, and low cost [Li06][Lin08b][Liu07]. Generally used polymer materials of ACAs are epoxies, silicones, acrylics, polyurethanes, cyanate esters, and polyimides [Lic05][Lin08b]. Both ACAs and NCAs are typically a mixture of epoxy polymer resins [Chi01][Lew08][Yim03]. The polymers of NCAs insulate electricity very well and have high break-down voltage [Liu99]. Adhesives should form robust bonds and have good adhesion to all surfaces involved in

the interconnections [Kwo06a][Li06][Lyo03]. To guarantee this, cleanliness of the bonding surfaces before bonding process should be confirmed.

The materials for conductive particles of ACA should also be considered when the adhesive for an application is selected [Li06][Lin08b]. The selection should be considered with a view to cost, electrical conductivity, current carrying ability, chemical reactivity, electromigration, corrosion and oxidation under heat and humidity conditions [Lin08b]. Typical materials used for conductive particles are silver (Ag), gold (Au), copper (Cu), nickel (Ni), aluminium (Al) and polymer particles with metal coating [Lew08][Li06][Lin08b]. The most widely used conductive particles are silver and nickel particles, and polymer particles with nickel or gold coating [Liu07]. In addition to the material choices, concentration and sizes of the conductive particles should also be considered in every application [Kwo06a]. The size of the particles in ACAs is typically 3-10 µm [Chi01][Hwa09][Kwo06a].

In addition to conductive particles, ACAs and NCAs may contain non-conductive particles, such as silica [Yim03][Yim07]. They are added to improve mechanical properties of the adhesives, such as lowering the coefficient of thermal expansion (CTE), and increase Young's modulus [Kim08b][Teh04][Yim03].

In this study an NCF, three ACFs and an ACP were used. They all were commercially available epoxy based thermosets. ACP had nickel particles of average 1.2 µm in diameter. Two ACFs had gold plated polymer balls as conductive particles with average 3 µm (ACF2) and 5 µm (ACF1) in diameter. The third ACF (ACF3) had gold coated nickel particles of average 8 µm in diameter. The ACF (ACF1) with larger polymer particles and the ACF with Nickel particles contained also non-conductive silica particles. They were added to lower its CTE, nevertheless, they also increased their Young's modulus. The size of silica particles was 0.8µm.

2.6 Advantages of ACAs and NCAs

Adhesives used in polymeric interconnections have numerous advantages over conventional solders with underfills. Furthermore, they are able to fulfil the requirements of today's electronics packaging. The trend in electronics packaging is towards miniaturization and therefore small and lightweight devices with better performance are sought [Lin08b]. With finer pitches packaging density can be increased [Lew08][Li05]. ACAs and NCAs can be used in very fine pitch applications, because the risk of electrical shorts is small [Li06][Lu10a][Tum97b]. Especially with NCA, the pitch can be extremely small as it is not limited by particle size or percolation phenomenon [Li06][Liu99][Tsa08].

In addition, electronics with lower cost is desired [Lew08][Yim03]. Polymeric interconnections can be used in more sensitive applications and with various substrates and components as the bonding temperature is lower than that in the soldering process [Kri98][Liu98a][Liu05][Lu10a][Yim03]. Consequently, low-cost components and substrates are also suitable [Cai08][Li06]. In addition, the bonding process of ACA and NCA has fewer processing steps because no underfill is needed [Liu05][Tum97b]. This more flexible and simpler process reduces processing costs [Li05][Li06][Liu05]. Moreover, due to the fewer processing steps production throughput increases [Wan08]. NCAs are even more cost-effective than ACAs because they do not contain conductive particles [Hwa09][Li06][Liu99][Tsa08][Yim03].

Polymeric interconnections are an environmentally friendly alternative to solders containing lead, flux or other harmful substances [Li06][Liu99][Lu10a][Wan08]. Additionally, the use of adhesives increases material options for the metallization [Li06] [Lin08a]. Furthermore, stress on the substrates and joints is smaller [Li06][Wan08] and the alignment of the adhesive is not so critical as the whole bonding area is covered with the ACA or NCA [Dob07][Kri98][Wan08].

2.7 Limitations of ACAs and NCAs

Although polymeric interconnections have numerous advantages, they have also some challenges and limitations which impedes the possibilities of using them as substitutes for solders in all applications [Li05][Li06]. Adhesive attachments have higher contact resistance, lower electrical conductivity, and more limited current-carrying capability than solders [Lew08][Li05][Li06][Yim99][Zho05a]. Additionally, adhesives have no self-alignment effect [Liu98b][Zho05a] and they have poor impact strength [Li05] [Li06]. Moreover, mechanical strength is lower, especially when they are exposed to different environments [Lew08].

The long-term reliability of the polymeric interconnections, especially in thermal and humid environments, is typically not as high as with solders [Lin08b]. Electrical performance as well as mechanical stability may deteriorate in demanding conditions [Li05][Li06][Liu98b]. Furthermore, uneven bonding surfaces or bump heights may cause uneven electrical performance and reliability between the joints [Lai96][Lyo03]. Moreover, in the bonding process of ACAs and NCAs, pressure together with heat is needed [Lew08]. Therefore the equipment for conditional solder reflow cannot be used in the bonding process of ACAs and NCAs [Liu98b][Zho05a].

2.8 Applications

Adhesives are suitable for numerous applications such as cell phones, radios, computers, personal digital assistants, digital cameras, memory chips and displays [Li06][Liu05][Yim06]. Although these adhesives are used widely in flip chip attachments, they are also suitable for surface mount technology, chip scale packaging (CSP) and flex on printed wiring board bonding [Li06][Liu98a][Liu05][Yim06]. Moreover, there is potential to use them even more widely [Liu98a][Lyo03].

One of the most common applications for adhesives, especially for ACA joints is flat panel display modules [Hwa09][Kri98][Liu05][Yim06]. The adhesives fulfil the requirements of the display modules, such as high resolution, light weight, thin profile and low power consumption [Wat04][Yim06]. Adhesive attachments can be used in liquid crystal displays (LCDs) in flex to printed wiring board bonding, and in direct chip attachments such as chip on flex (COF) and chip on glass (COG) [Hwa09][Wat04] [Yim06]. Moreover, in plasma display panels (PDPs), and organic light-emitting diodes (OLED) ACAs are used to attach driver IC to glass substrate using tape carrier packages (TCPs) [Yim06]. The advantages of the adhesives compared to solders in these applications are low cost, fine pitch capability and low assembly temperatures [Kri98] [Lyo03][Wat04].

Polymeric interconnections are also widely used in various flip chip applications. By using flip chip technique instead of other bonding techniques, high joint density, low parasitic capacitance and inductance, and low joint resistance are achieved [Kim08b]

[Lau98a]. In addition, flip chip technique meets the demands of higher packaging density, as a result of the high electrical performance together with smaller, lighter and thinner package [Kim08b][Yim06]. When ACAs are used in flip chip joints instead of solders, lower processing temperatures, shorter processing times and lower costs are achieved [Li06][Yim06].

2.8.1 Radio frequency identification

ACAs are also suitable for high frequency applications and consequently, one significant application for ACA flip chip joints is radio frequency identification tags (RFID tags) [Ras04][Yim06]. RFID is a fast developing technology in the field of identification and security [Nik06][Rao05]. RFID tags can be effectively used in various applications [Dom07][Nat06][Rao05]. For example, they can be used to identify and track products during the manufacturing, distribution and shipment of a device [Rao05][Ras04]. Tags are used successfully in various industries, such as aeronautics, automotive and medicine [Dom07][Nat06].

RFID uses radio waves in the identification of physical objects from distances up to several meters with passive RFID systems [Dob07]. With RFID tags it is possible to identify objects individually and reliably, and multiple objects can be identified simultaneously without human assistance. Compared to bar codes, RFID tags are more durable in demanding conditions and no visual connection between a reader and a tag is needed. [Wan06]

A tag consists of an antenna which receives and backscatters radio frequency signals and a microchip which controls the operation [Dob07]. ACAs are widely used to attach microchips to RFID antennas with flip chip technique especially due to the low processing temperatures and low costs [An07][Cai08]. Low processing temperatures enable the use of low cost substrates commonly used in RFID tags [Cai08].

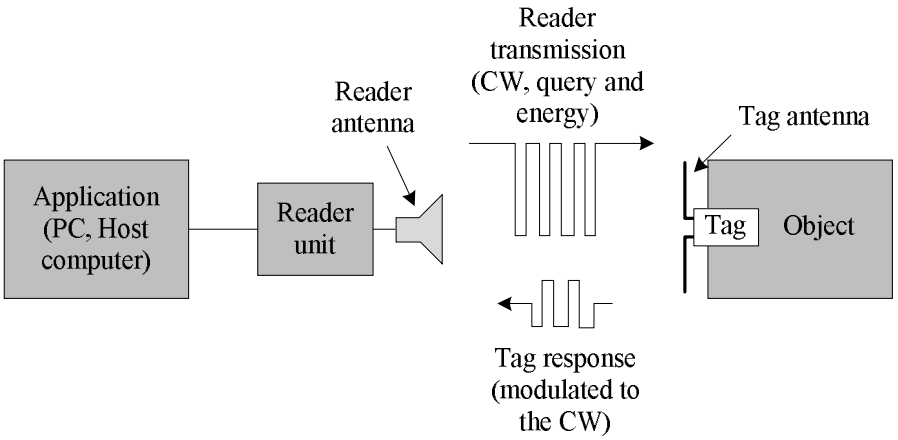

Figure 5: Components and operational principle of a passive UHF RFID system. [Dob07]

An RFID system consists of a reader and a tag. The reader transmits radio wave signals to the tag which replies by backscattering a modulated signal which contains its identification code. [Wan06] Ultra high frequency (UHF) radio frequency identification tags operate at frequencies from 860MHz to 960MHz. Tags, which draw their operating energy from the radio waves emitted by a reader instead of having internal energy source, are called passive tags. [Dob07] The components and the operating principle of

a passive UHF RFID system are presented in Figure 5. Passive UHF RFID tags suit numerous applications, because they are inexpensive, compact, mechanically robust, and their read range is several metres [Dob07].

2.9 Test samples

As ACAs and NCA are commonly used in flip chip joints in various applications, flip chip joints were also studied here. In Publications I, IV, V and VI bare test chips were attached onto substrates. In Publications II and III UHF RFID tags were used as test samples.

In Publication I six test lots with different structures were made using two different ACFs, three different test chips and four different FR-4 substrates. Three of the substrates were bare FR-4 with thicknesses of 100 µm, 600 µm and 710 µm, and the fourth was a 710 µm thick FR-4 with a resin-coated copper foil (RCC) laminated onto it. The size of all three test chips was 5 mm x 5 mm and they had 69 bumps which were located peripherally with a pitch of 250 µm. Thicknesses of the chips were 500 µm, 480 µm and 80 µm. The chip with thickness of 500 µm had gold bumps, while the other two chips had copper bumps. The six test lots with different combinations of the substrates, ACFs and chips are listed in Table 1.

Table 1: Test lots with different thicknesses of chips and substrates.

	Chip	**ACF**	**Substrate**
Test lot 1	480 µm	ACF3	710 µm
Test lot 2	480 µm	ACF3	100 µm
Test lot 3	80 µm	ACF3	710 µm
Test lot 4	480 µm	ACF3	710 µm + RCC
Test lot 5	500 µm	ACF2	600 µm
Test lot 6	500 µm	ACF2	100 µm

In Publications IV and V flip chip joints with NCF were made using a 100 µm thick FR-4 substrate and a ceramic 635 µm thick alumina (Al_2O_3) substrate. The test chips were silicon chips with dimensions of 5 mm x 5 mm x 500 µm, and they had 69 gold stud bumps which were located peripherally with a pitch of 250 µm.

In Publication VI flip chip joints were made using two different ACFs; ACF1 and ACF2. The substrate was 100 µm thick FR-4 and test chips were silicon chips with dimensions of 5 mm x 5 mm x 500 µm and they had 69 gold bumps located peripherally with a pitch of 250 µm.

In Publications II and III a passive UHF RFID tag was used as a test sample. Its microchip was attached using the ACP. The tag was manufactured on a 50 µm thick polyethylene terephtalate (PET) substrate and the metallisation on in was 9 µm thin aluminium. The tag antenna was a dipole whose length was roughly 11cm. A photograph of the test tag is shown in Figure 6. The microchip in the middle of the tag was a silicon chip with dimensions of 760 µm x 760 µm x 150 µm. The chip had four gold bumps, one in each corner.

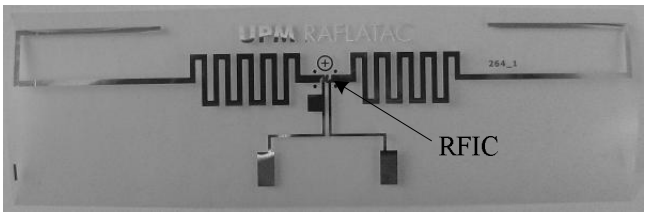

Figure 6: Test tag.

The bonding parameters used in this study are listed in Tables 2 and 3. The parameters of NCF with both substrate materials and all three ACFs are listed in Table 2. They were chosen according to recommendations of the adhesive manufacturers. Four different bonding pressures were used in ACF joints in Publication I and two different pressures in Publication VI to examine the effect of pressure on the reliability. In addition, the bonding parameters of ACP joints were also varied to observe the effects of the changes in them on the reliability. Four different test series with different bonding parameters were prepared and they are listed in Table 3. They were chosen by the manufacturer of the RFID tags.

Table 2: Bonding parameters of NCF with different substrates and ACFs.

	NCF + Al_2O_3	**NCF + FR-4**	**ACFs**
Pre-bonding			
Temp. of tool [°C]	90	90	90
Temp. of table [°C]	70	70	70
Heating time [s]	10	10	10
Pressure [MPa]	1	0.5	0.5
Bonding			
Temp. of tool [°C]	230	200	220
Temp. of table [°C]	100	100	100
Heating time [s]	15	25	25
Cooling time [s]	15	15	15
Pressure [MPa]	100	100	50, 80, 110, 140 (Publication I) 80, 110 (Publication VI)

Table 3: Bonding parameters of ACP.

Series	**Temperature of the tool [°C]**	**Temperature of the table [°C]**	**Pressure [N]**	**Heating time [s]**
A	190	170	0.75	7
B	190	170	1.3	7
C	200	160	0.75	7
D	200	160	0.75	10

3 Reliability of ACAs and NCAs

Inadequate reliability data on polymeric interconnections in various environments is one of the limitations which have inhibited the wider use of polymeric interconnections as a replacement for solders [Liu98b][Teh04][Wan09][Yim03]. Reliability is typically defined as the probability of a product to perform a required function without failure under given conditions for a given period of time [Jen95][Ohr98][Suh02]. The reliability requirements of a product depend largely on the application. The demands for reliability in applications in medical, military or avionic electronics are extremely high, as human lives may depend on the electronics. On the other hand, in consumer electronics electrical failures are typically bothersome and cause loss of money, but danger to users is unusual. [Tum01] In any case, in every application reliability needs to be taken into account during design and manufacture. Nowadays electronics is exposed to various environments during manufacturing, shipment and operation. Nevertheless, the reliability requirements of the products need to be fulfilled even in demanding conditions. [Tum01]

3.1 Accelerated life testing

Accelerated life test (ALTs) are generally used to study the effects of environmental conditions on the reliability [Jen95][Suh02]. In ALTs products are exposed to stresses which they are also assumed to be exposed to during their lifetime [Jen95]. However, the tests are accelerated by elevating stress levels thus the failures occur over a much shorter period of time [Bro99][Jen95][Suh02]. ALTs are used to detect possible failure modes and mechanisms, and to accumulate reliability statistics [Suh02]. However, if too harsh a test is chosen, the failure modes and mechanisms may not be the ones which would occur in the operating conditions of the product and the test will not illustrate the performance in the operating environment [Jen95][Suh02].

When the stresses for an ALT are chosen, the proposed application and its operational environment need to be well known [Tum01]. The stresses may, for example, be constant or varying temperature or humidity, mechanical shock or vibration, corrosive environment, or extreme voltages [Suh02]. In earlier studies on polymeric interconnections, the combined effects of thermal and humidity stresses have been found to be most important for the failures [Lah06][Lin08b][Lai96][Lin08b][Yim99] [Zho05b]. However, in some applications mechanical stresses may be the most critical for reliability and also merit careful consideration when reliability of polymeric interconnections is determined [Mor07].

The polymer based joints are vulnerable to moisture sorption and expansion [Lin08b]. As the chip, metals and ceramics around the joints are not expanding as much, stress will be induced in the joints [Lau98b][Teh05][Yin05a][Zho05b]. Similar effect occurs also when polymer expands or contracts in thermal environments more than the other material around it [Kwo06b][Yin03]. Consequently, polymeric interconnections are tested typically in high temperature and humidity tests, and in temperature cycling tests [Cha00][Kri98][Lai96][Lin08b][Saa08][Teh04][Yim99][Yim03]. This study has also been limited for thermal and humidity stresses.

In this study a constant humidity test, a humidity cycling test, constant temperature tests and thermal cycling tests were used. The constant humidity test was performed

according to standard EIA/JESD22-A101-C [Jed09a]. Temperature and relative humidity were chosen to be 85 °C and 85 %RH. The constant humidity test was used for NCF samples with both substrates and for the RFID tags (Publications III, IV and V). The tags were tested for 2,000 hours, the NCF joints with ceramic substrate for 2,500 hours, and the NCF joints with FR-4 substrate for 4,000 hours.

The RFID tags in Publication III were also tested using a humidity cycling test where relative humidity changed from 10 %RH to 85 %RH and temperature from 25 °C to 85 °C. Humidity level was fluctuated from 10 %RH to 85 %RH while temperature was kept at 85 °C. The exposure time at both humid conditions was 2 hours. The total cycling time was 8 hours and the cycle profile is shown in Figure 7. The transition time from high humidity level to low humidity level was 40 minutes, while the transition from the low level to high level was 3 hours and 20 minutes. The times were different because the temperature was dropped to room temperature for a while, when the humidity level was raised from the lower level to higher level. This was done to amplify the harshness of the test. The humidity cycling test was not based on any test standard. The tags were tested for 504 cycles.

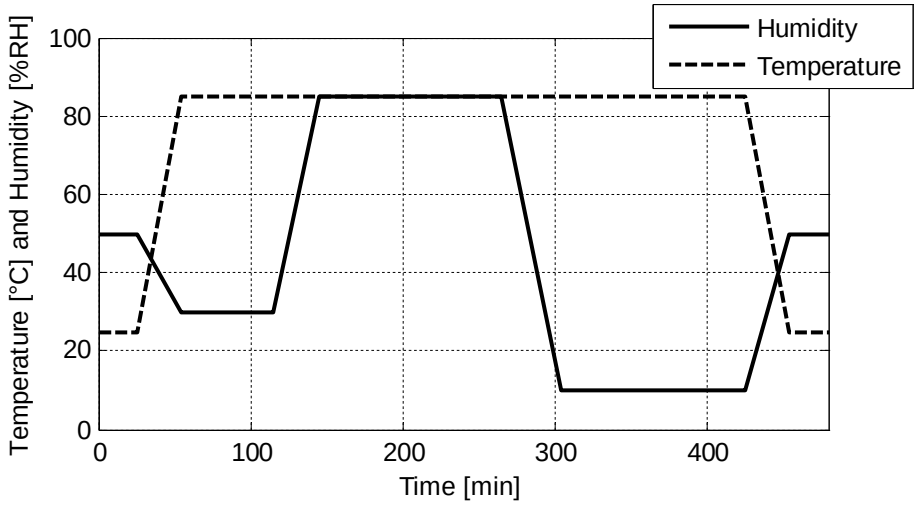

Figure 7: Profile of a cycle in the humidity cycling test.

Additionally, the ACP joints of RFID tags were tested using two different temperature cycling tests with temperatures varying from -40 °C to 85 °C and from -40 °C to 125 °C (Publication II). The tests were conducted according to Standard JESD22-A104D [Jed09b]. In both tests, the exposure time at extreme temperatures was 14 minutes and the transition time was 1 minute. Thus the total cycling time was 30 minutes. The tags were tested for 3,000 cycles in the -40 °C to 85 °C test and for 2,500 cycles in the -40 °C to 125 °C test. The ACF joints in Publications I and VI were also tested in the -40 °C to 125 °C test. Duration of the test for ACFs was 10,000 cycles.

The high temperature tests were used to test the reliability of RFID tags in Publication II. The temperatures were the same as the upper extreme temperatures in the temperature cycling tests, i.e. 85°C and 125°C. The duration of the test at the temperature of 125°C was 3,000 hours while the duration of test at the temperature of 85°C was 1,000 hours.

3.2 Test evaluation methods

To be able to define failures, an indicator for the performance of the product and failure criterion needs to be defined [Ohr98]. The indicator should be a factor which describes the performance of the product, and it needs to be measurable [Jen95]. The failure criteria express the performance limits inside which the device has to perform, or otherwise they are deemed to have failed [Ohr98]. Both of these are heavily dependent on the product and the application [Jen95][Ohr98]. The selection of failure criterion may have a significant effect on the reliability results and therefore it is important to define it according to the application and meaning of the reliability test [Kok10][Liu07]. When the aim of the test is to find the root cause of failure or failure mechanisms, it is often beneficial to have higher failure criterion [Kok10].

3.2.1 Resistance

Contact resistance describes the electrical properties of joints and is a good indicator of the quality and reliability of ACA and NCA joints [Cae04][Liu07][Sep04]. Consequently the contact resistance is widely used to monitor the reliability during environmental testing [Cae04][Hwa09][Kok10][Liu07][Sep04][Udd04]. Especially in temperature cycling tests, it is possible that the changes in contact resistance may occur during the test in extreme conditions but not at room temperature after testing [Hua10] [Sep04]. This kind of behaviour was observed in the temperature cycling tests in this study. Therefore a continuous real time measurement during the testing is necessary [Sep04].

Continuous real time resistance measurement was used in this study for all other test samples except for the RFID tags in the humidity tests. All the test chips included a daisy chain structure and the daisy chain resistances were measured. In daisy chain structure the joints are connected in series via electrical wirings in turns between adjacent bumps or adjacent pads. The idea of daisy chain structure is illustrated in Figure 8.

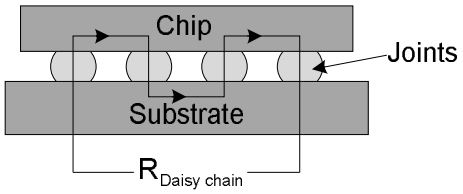

Figure 8: Idea of daisy chain structure.

In the real time measurements of this study, each sample was in series with a constant 1000Ω resistance and there was a supply voltage over them. The voltages over samples were monitored and the values of measured voltages were converted into relative values of resistances. Circuit diagram of the measurement system is shown in Figure 9. The measurements were made every 20 seconds.

Three different failure criteria in resistance measurements were used. In Publications IV and V open joint, in Publication II at least ten-fold increase in daisy chain resistance, and in Publications I and VI at least doubling of the daisy chain resistance were chosen as the failure limits.

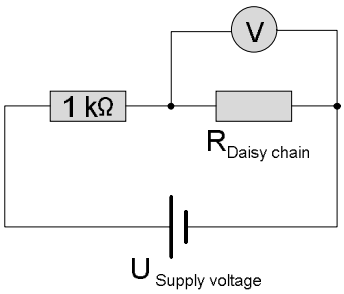

Figure 9: Circuit diagram of real time daisy chain resistance measurement system.

3.2.2 Adhesion

In addition to resistance, adhesion is another important factor describing changes in the joints during environmental testing [Hwa09][Teh04][Udd04]. Materials with physically and chemically different properties are commonly combined in electronic applications [Tur04]. Nevertheless, the adhesion between these materials should withstand exposures to different environmental conditions during assembly, handling and lifetime [Tur04] [Udd04]. Consequently, adhesion strength is a critical parameter in polymeric interconnections [Udd04]. Adhesion forces hold the joint surfaces in contact and adhesion strength describes mechanical properties of the joints [Lic05]. Adhesion is caused by interactions at surfaces which may be physical, chemical, mechanical or frictional [Ast06].

According to earlier studies, the adhesion of material interfaces may weaken during environmental testing and cause long-term failures [Lin05][Lin06a][Lin06b][Luo05] [Teh04][Teh05][Tur04]. In addition to the mechanical degradation of the joints, lack of adhesion also has an effect on the electrical properties of the joints in polymeric interconnections [Riz05][Tur04]. Impaired adhesion strength together with environmental stresses may cause delamination on bonding surfaces, cracking of the materials, or open joints [Luo05][Teh04][Tur04].

Adhesion is typically tested using shear tests or pull-off tests [Hwa09][Lin06b][Luo05] [Teh04][Tur04]. In pull-off tests the pull force to the joints is applied vertically in z-direction [Hwa09][Tur04]. On the other hand, in shear tests the force is applied horizontally on an xy-plane [Lin06b][Luo05][Teh04]. In adhesion tests of adhesive joints, three types of failure modes may occur. Adhesion failure indicates separation of joint surfaces, breakage in a bulk material is a sign of a cohesion failure, and in mixture failure both of these two failure modes will occur. [Lin06b]

In this study, the effect of humidity on the adhesion of NCF joints with two different substrate materials was studied in Publications IV and V. The samples were tested in the constant humidity test for different time periods and after testing an adhesion strength test was made using a shear test. In Publication IV, the adhesion strength tests for NCF joints with ceramic substrate were continued for 2,500 hours at intervals of 500 hours in the humidity test. In Publication V, the adhesion tests for NCF joints with FR-4 substrate were conducted after 500, 2,000 and 4,000 hours. In the shear test, the substrate was held still while the test chip was pushed horizontally from one side. The pushing force needed to separate the chip from the substrate was measured. The operating principle of the adhesion strength test is presented in Figure 10.

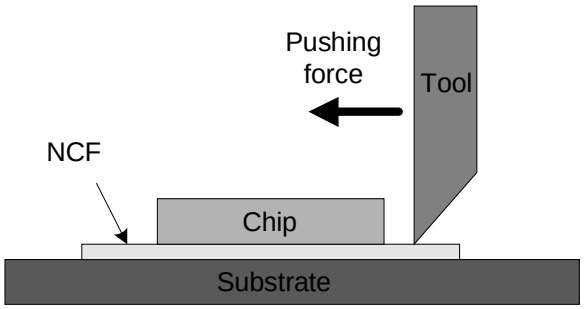

Figure 10: Operating principle of adhesion strength test.

3.2.3 Threshold power measurements

When RFID tags are tested, changes in performance parameters may also be used as an indicator of reliability. The most important performance characteristic is read range, which describes the maximum distance between a reader and a tag at which the reader can detect the backscattered signal from the tag [Rao05][Ras04]. Theoretical read range can be calculated on the basis of threshold power measurements [Rao05]. Threshold power is the minimum transmitted power from the reader antenna to activate the tag and to receive a response to ID query at a certain frequency and a distance [Dob07].

In Publication III the changes in the RFID tags during the humidity tests were observed by measuring the threshold power after different periods in the tests. The tags were tested within a frequency band from 800 MHz to 1 GHz using 1 MHz steps with customized RFID measurement equipment. The measurements were carried out in a compact measurement cabinet where the distance between the reader antenna and the tag was 0.45m. The gain of the measurement antenna was 8.5dBi. The threshold power sweeps after different periods in humid conditions were compared to identify any significant changes in the performance parameters of the tags. The tags were deemed to have failed when the threshold power doubled at the optimal operating frequency. For the tags in the constant humidity test, the measurements were made after each 500 hours. For the tags in the humidity cycling test, the measurements were initially conducted after every 21 cycles until 168 cycles was reached. They were then conducted after every 42 cycles until 420 cycles was reached, and finally after 84 cycles until 504 cycles was reached.

3.3 Analysis of the results

As ALTs are used to detect possible failure modes and mechanisms, and to accumulate reliability statistics [Suh02], failure times, modes and mechanisms need to be analysed after testing. Statistical methods are used in the estimation of failure times [Bro99] [Oco01][Jen95][Ohr98][Tum97a]. A distribution which fits the test results is sought and the parameters of that distribution are defined [Bro99][Tum97a]. Failure modes are observed as changes in the performance of the product, whereas failure mechanisms are the processes which cause the failures [Jen95].

3.3.1 Statistical analysis

After testing the failure percentages of the results of a reliability test can be plotted as a function of time. Although the number of samples is finite, the results may tend to be a continuous distribution which is called a probability density function (PDF), *f(t)* [Oco01][Ohr98]. Generally used distributions in reliability studies of electronics are

normal, exponential, log-normal and Weibull distributions [Jen95][Ohr98]. They all have different PDFs and parameters which describe the shape of a distribution [Bro99] [Jen95][Ohr98].

Weibull is a versatile distribution which has been used to study the reliability of ACA interconnections [Kwo05][Liu02][Liu07]. It is also used in this work for statistical analysis of the reliability tests. PDF of a two-parametric Weibull distribution is:

$$f(t) = \frac{\beta}{\eta}\left(\frac{t}{\eta}\right)^{\beta-1} e^{-\left(\frac{t}{\eta}\right)^{\beta}} \quad (1)$$

where η is a scale parameter and β is a shape parameter. The scale parameter η is a life-point value and gives the age at which 63.2% of the test samples failed. The shape parameter β defines the shape of a distribution. With $\beta < 1$ the distribution has a failure rate that decreases over time. On the other hand, when $\beta > 1$, the failure rate of the distribution increases over time. With $\beta = 1$ the failure rate is constant. [Bro99][Jen95] [Tum97a]

The scale and shape parameters are used to compare the reliability between different test series. The scale parameters are used in the comparison of failure times and the shape parameters describe the divergence in failure times between the test samples. Significant difference in shape parameters between test series may indicate different failure mechanisms.

3.3.2 Failure Modes

Failure mode is the effect in the performance of the product by which a failure is observed [Oco01][Jen95]. Since the resistance of polymeric interconnections is widely used as an indicator of performance, the changes in the resistance are interpreted as failure modes [Fri06b][Sep04]. In this study resistance and threshold power measurements were used as indicators of the performance of the samples and consequently, changes in these indicators were also interpreted as failure modes. Failure modes of electrical devices may be categorized to four classes; short circuit, open circuit, degraded performance and functional failure [Jen95]. In this study two types of these failure modes were observed; open circuit and degraded performance.

3.3.3 Failure Mechanisms

Different failure modes may indicate different failure mechanisms [Fri09][Sep04]. A failure mechanism is the process which causes the failures [Bro99][Oco01][Jen95]. The process may be chemical, physical or mechanical [Bro99][Jen95][Tum01]. There are many factors which may cause conducting failures of polymeric interconnections and in practice different factors may act simultaneously [Lai96]. Some of the failure mechanisms may be observed visually such as open joints, delamination or cracks [Lai96][Liu11][Teh04][Tur04]. On the other hand, adhesive joints may also fail due to relaxation, metal oxidation or degradation of the polymer matrix, which may be difficult to detect visually [Cha00][Lai96][Liu98b].

Different expansions of polymers compared to those of metals or ceramics in thermal or humid environments can cause failures in different ways. These different expansions may decrease the contact area or cause an open joint [Cha00][Kri98][Lai96][Teh04].

They may also cause stress to the structure which may be released by cracking or delamination [Lai96][Lew08][Liu98b]. Additionally, differences in the expansions of the polymer matrix and conductive particles can cause conductive gaps to ACA joints [Lai96][Yim99]. The expansion of polymer matrix is more critical when ACAs with rigid particles instead of metal coated polymer particles are used [Sep04]. Moreover, mismatch in the expansion of chip and substrate may cause the structure to warp which may decrease the compressive forces holding the joints in contact [Kim08b][Sep04] [Wan08]. This mismatch may also cause shear stress into adhesive and its interfaces.

In humidity tests delamination may also be induced due to water seepage at the material interfaces [Cha00]. In addition, an insulating oxide layer may be formed on the bonding surfaces and around the conductive particles in humidity tests [Cha00][Kri98][Lai96] [Liu98b][Liu07][Mub09][Yim99]. Aluminium, copper and nickel are especially prone to oxidation [Cha00][Mub09][Yim99].

During environmental testing, relaxation may occur in the polymer matrix when the compressive forces, which have formed to the joints during the bonding process, are released [Lai96][Sep04][Teh04][Tur04]. The relaxation is more significant if the glass transition temperature (T_g) of the adhesive is exceeded during testing [Cha03][Kwo04a] [Sep04].

Material degradation of ACA has also been found to be one reason for failures [Lai96] [Lin06b][Liu07]. Hygrothermal aging especially causes chemical and mechanical changes to epoxy based polymers, which do not recover after testing [Lin06a][Lin06b] [Liu98b][Mub09]. During hygrothermal aging T_g of the material decreases, hydrolysis may undermine the mechanical properties, plasticization may soften polymer, adhesion and cohesion may decrease as a function of time, and bond strength may decrease [Lai96][Lin06a][Lin06b][Mub09][Yim99]. Additionally, conductive particles may move due to expansion of the polymer matrix [Cha03]. This movement may be significant especially at testing temperatures above T_g temperature when the polymer matrix turns from hard and solid state to soft and rubbery state [Cha03][Tum01]. Moreover, the properties of the joints may change during testing as adhesives continue curing in the tests with raised temperature [Lin06a][Udd04].

In this study failure mechanisms and places were examined using scanning electronic microscope (SEM). Cross-sections of some of the failed samples were made to expose contacts. Additionally, in Publication III the metallization of tested RFID tags were examined with an optical microscope to find any cracks which may have affected on the performance of the tags.

3.4 Thermal tests

In this study, comparisons of the reliability of different test structures in the same thermal test and same test structures in different thermal tests were conducted. The results of the thermal tests are presented in this chapter. Firstly the test structure was varied by comparing two different ACF materials in a temperature cycling test. Additionally, test structures with the same materials, but different thicknesses of the substrate and the chip were tested. Furthermore, RFID tags were tested in different thermal tests and the results were compared.

3.4.1 Comparison of ACF materials

In Publication VI, an ACF with silica (ACF1) and an ACF without silica (ACF2) with two different bonding pressures were tested in a temperature cycling test where temperature varied from -40 °C to 125 °C. The Weibull plots for the results are shown in Figure 11. Numbers of failed samples (F), numbers of censored samples (C), the shape parameters (β), and the scale parameters (η) of Weibull distributions are listed in Table 4. When the samples with the same bonding pressures but different adhesives were compared, the joints with ACF1 were found to be more reliable than those with ACF2. In addition, joints with both adhesives were more reliable when they were bonded with the higher bonding pressure.

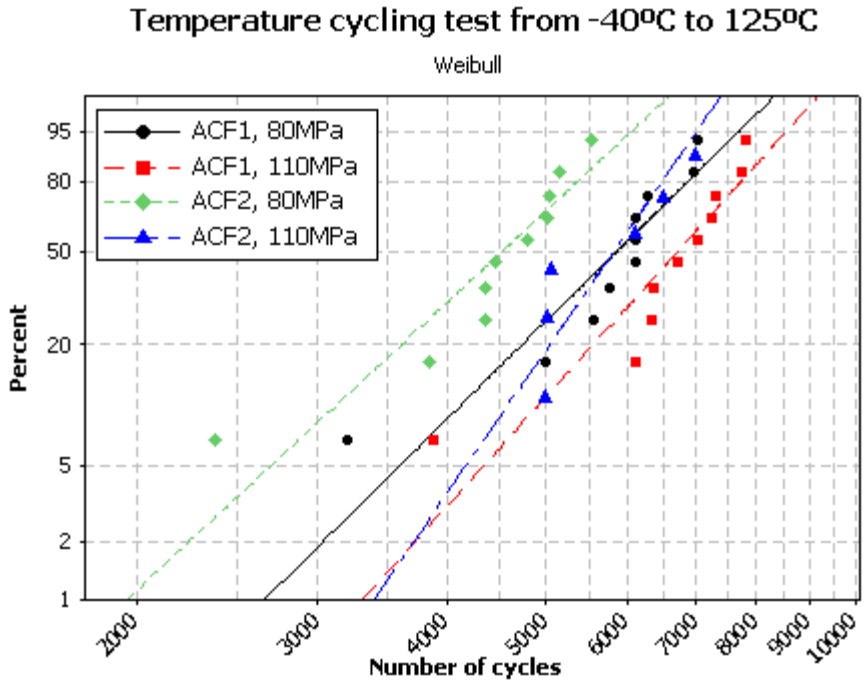

Figure 11: Results of comparison of ACFs in temperature cycling test.

Table 4: Table of statistics of comparison of ACFs in temperature cycling test.

	β	η	F	C
ACF1, 80MPa	5.368	6,269	10	0
ACF1, 110MPa	6.013	7,133	10	0
ACF2, 80MPa	5.047	4,867	10	0
ACF2, 110MPa	7.908	6,090	6	0

Although the failure modes were similar, a difference was observed in the failure mechanisms. Delamination between bump and pad, and cracking of the substrate were found in every test sample studied with ACF1. Similar cracking of the substrate was also found from every test sample with ACF2. However, in the majority of the failed test samples with ACF2 no delamination between the pad and the bump was found. It is likely that the delamination caused the failures in the test samples with ACF1. However, the reason for the failures in the test samples with ACF2 is probably the deformation of the adhesive matrix during testing, which eventually caused the conductive particles to lose contact and the joint failed. In the failure analysis it was observed that the

delamination causing the failures was typically found in the corner joints or in the nearby joints.

3.4.2 Comparison of chip and substrate thicknesses

In Publication I the effect of thicknesses of substrate and chip on the reliability were tested using the temperature cycling test from -40 °C to 125 °C. Six test lots with different structures were made using two different ACFs, three different test chips and four different FR-4 substrates. The six test lots with different combinations of the substrates, ACFs and chips are listed in Table 5. Four different bonding pressures; 50 MPa, 80 MPa, 110 MPa and 140 MPa were used in each test lot to investigate its effect on the reliability.

Table 5: Test lots with different thicknesses of chips and substrates.

	Chip	ACF	Substrate
Test lot 1	480 µm	ACF3	710 µm
Test lot 2	480 µm	ACF3	100 µm
Test lot 3	80 µm	ACF3	710 µm
Test lot 4	480 µm	ACF3	710 µm + RCC
Test lot 5	500 µm	ACF2	600 µm
Test lot 6	500 µm	ACF2	100 µm

In the test results a clear difference was observed between the test lots. Weibull distribution was used to analyse the results statistically. The shape parameters (β) of the different test lots with the different bonding pressures are shown in Figure 12 and the scale parameters (η) in Figure 13. When the scale parameters are compared, test lot 1 was observed to have the lowest reliability. Test lot 2, which had thinner substrate compared to test lot 1, had clearly improved reliability. Similarly, test lot 6 had thinner substrate than test lot 5, and test lot 6 was also more reliable than test lot 5. Hence, the thinning of the substrate was observed to improve reliability. Likewise, the thinning of the chip seem also to improve the reliability, as test lot 3 which had thinner chip compared to test lot 1, had better reliability than test lot 1. When the scale parameters of test lots 1 and 4 were compared, the addition of RCC layer onto the substrate also seems to improve the reliability.

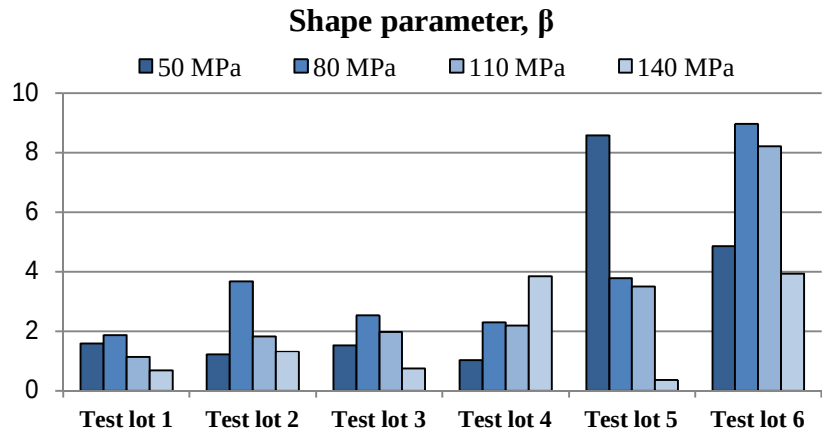

Figure 12: Shape parameters (β) of different test lots with different bonding pressures.

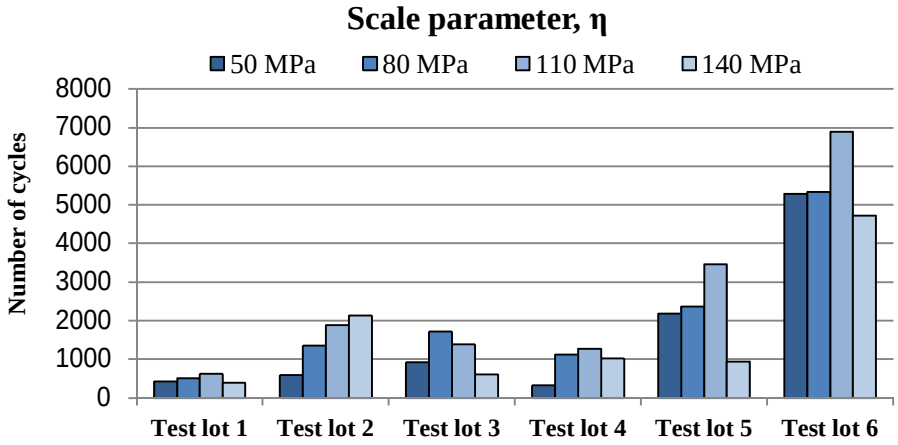

Figure 13: Scale parameters (η) of different test lots with different bonding pressures.

The failure modes of the samples with the three highest bonding pressures were similar. The increase in daisy chain resistance was generally observed at the stage of a cycle during temperature changes, or at the low extreme temperature. However, later the resistance also increased at high extreme temperature. On the other hand, in most of the samples with lowest bonding pressure, daisy chain resistance increased first at the high extreme temperature. In the failure analysis, delamination in the joints and cracking of the substrate were observed in most of the test samples. [Fri06a][Fri07a][Fri07b] Delamination was observed at the corner joints or nearby joints. The location of the failure was dependent on the location of the glass fibres in the FR-4 substrate. The distance of the glass fibres of the FR-4 substrate to the surface in the FR-4 substrate varied, and consequently the layer of epoxy between the pads and glass fibres varied according to the location of the pad on the substrate. When the fibres were near the surface, they supported the joints and improved their reliability. On the other hand, a thick layer of epoxy under a pad deformed during the bonding process and made such joints more susceptible to failures. If there was such variation in the corner areas of a chip, it was seen that the failures occurred in the joints near the corner having a thick layer of epoxy instead of at the corner joints. However, if no variation was present or if the corner joints had a thick layer of epoxy, failures were detected in the corner joints. In addition, there were also failed samples whose failure mechanism was not ascertained in SEM examination and it was assumed that they failed due to relaxation of the adhesive.

3.4.3 Comparison of thermal tests

In Publication II, four different test series of RFID tags with ACP were tested using two different temperature cycling tests and two different constant temperature tests. In the constant temperature tests with temperatures of 85 ºC and 125 ºC no failures were detected, even though the duration of the 125 ºC test was two times longer than the duration of the longer temperature cycling test [Saa10a]. However, in the -40 °C to 125 °C temperature cycling test all test samples and in the -40 °C to 85 °C test most of the test samples failed. The Weibull plots of the results of the temperature cycling tests are presented in Figures 14 and 15 and the statistics is listed in Table 6.

The results of the Weibull distributions show a clear difference between the temperature cycling tests [Saa10a]. The test samples in the -40 °C to 125 °C test failed significantly faster than the test samples in the -40 °C to 85 °C test. In addition, there was a

difference in the behaviour of the different test series. In the -40 °C to 85 °C test the samples in each test series failed quite evenly during the test. On the other hand, in the -40 °C to 125 °C test samples with higher bonding pressure were clearly more reliable than the others, as test series B had significantly higher scale parameter than the other test series. In addition, a clear difference in the shape parameters of the Weibull distributions between the tests was observed. The differences in the behaviours of test series and in the shape parameters may indicate different failure mechanisms between these two tests.

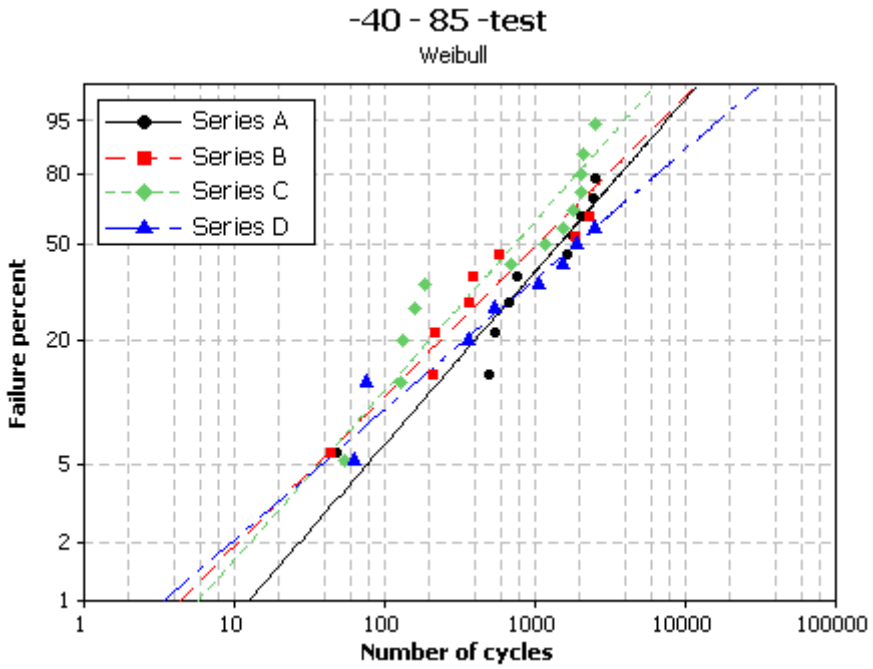

Figure 14: Results of ACP joints in the temperature cycling test where the temperature varied between -40°C and 85°C.

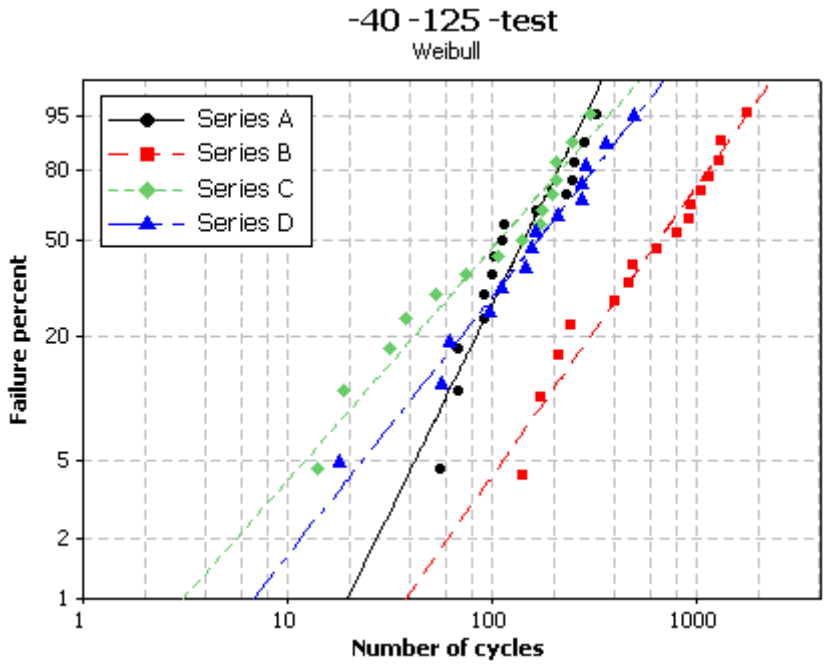

Figure 15: Results of ACP joints in the temperature cycling test where the temperature varied between -40°C and 125°C.

Table 6: Table of statistics of ACP joints in temperature cycling tests.

	-40 °C to 85 °C test				-40 °C to 125 °C test			
	β	**η**	**F**	**C**	**β**	**η**	**F**	**C**
Series A	0.89	2144	10	2	2.13	170	15	0
Series B	0.77	1634	8	4	1.48	837	16	0
Series C	0.88	1097	13	0	1.19	147	15	0
Series D	0.67	3171	8	5	1.32	220	14	0

Different failure modes in the temperature cycling tests were observed. In the -40 °C to 125 °C test the resistance increase was initially observed at the high temperature extreme. It took some time before the resistance increase was also observed at the low temperature extreme. On the other hand, in the -40 °C to 85 °C test the resistance increased simultaneously at both temperature extremes.

After testing the resistances of the test samples were measured again at room temperature. It was observed that the resistance values of the majority of the failed test samples had fallen below the failure limit. Thus, although the samples failed during testing, they were still working at room temperature after testing. This recovery made determination of failure mechanisms difficult. No delamination or cracks were seen in the test samples. However, an ACA joint may fail by many different mechanisms, which are typically detectable in SEM examination. In a thermal environment the ACA matrix expands markedly compared to the conductive particles [Lai96]. The expansion may push the particles away from the contacts and an open joint will form or at least the contact resistance will increase. If such expansion is mainly elastic, the increased resistance values may return close to the resistance values after testing. It is likely that the failures in the samples were caused by this kind of expansion and also by relaxation of the ACA matrix as they both may be critical mechanisms with rigid particles [Cha03] [Lai96].

3.5 Humidity tests

In this study humidity tests were used in the reliability study in two different ways, first by investigating the effects of different humid environments on reliability using one type of test samples in two different humidity tests, and second by measuring the effect of long-term exposure of humidity on the adhesion of the polymeric interconnections. The results of the humidity tests are presented in this chapter.

3.5.1 Comparison of humidity tests

In addition to the comparison of the thermal tests, the effects of two different humidity tests on reliability were also compared. In Publication III RFID tags with four different bonding parameters were tested using constant humidity test and humidity cycling test, and the results were compared. In the humidity cycling test most of the test samples failed. The Weibull plot of the results is shown in Figure 16 and statistics of the Weibull distribution are listed in Table 7. Series A and D seemed to be more reliable in this kind of test than series B and C. In addition, there is a clear difference in the shape parameters between the test series, thus it is possible that test series B and C had different failure mechanisms from test series A and D.

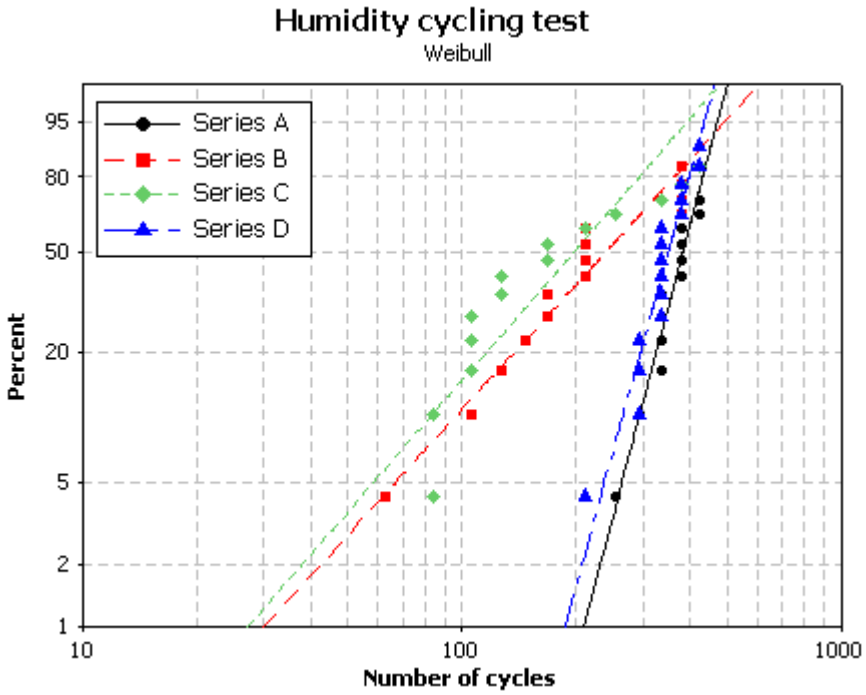

Figure 16: Results of the humidity cycling test.

Table 7: Table of statistics of ACP joints in humidity cycling tests.

	β	η	F	C
Series A	7.055	401	12	4
Series B	2.041	286	14	2
Series C	2.139	234	14	2
Series D	6.727	368	15	1

When the results of the humidity cycling test were compared to the results of the constant humidity test, significant differences were observed. The tags failed faster in the humidity cycling test and the effects of bonding parameters on the reliability were different. In the constant humidity test only four test samples failed during the 2,000 hour test and they were from test series D [Saa10b]. The numbers of failed samples in the constant humidity test compared to the total number of samples in each test series are shown on the left in Table 8. On the right of Table 8 are the corresponding numbers of cycles from the humidity cycling test and also the numbers of the failed samples compared to the total number of samples in each test series. The corresponding numbers of cycles were chosen from the measurement data so as to be as close as possible to the hours in the constant humidity test. The testing hours in the humidity cycling test are shown in brackets after the numbers of the cycles.

Different failure modes were also observed in the threshold power measurements between the humidity tests. In the humidity cycling test the tags failed by four different processes; they no longer activated at the frequency band, they activated only at the high frequencies with high threshold power, threshold power and optimal operating frequency increased significantly, or threshold power increased at optimal operating frequency so that the failure limit was exceeded. The first one occurred mainly in the

tags from test series B and C, while the last one mainly occurred in test series A and D. The samples in the constant humidity test failed in the two middle modes.

Table 8: Numbers of failed samples compared to the total number of samples in the humidity tests.

Constant humidity test	Series A	Series B	Series C	Series D	Humidity cycling test	Series A	Series B	Series C	Series D
1,000h	0/16	0/16	0/16	1/16	126 (1,008h)	0/16	3/16	7/16	0/16
1,500h	0/16	0/16	0/16	3/16	168 (1,344h)	0/16	6/16	9/16	0/16
2,000h	0/16	0/16	0/16	4/16	252 (2,016h)	1/16	10/16	11/16	1/16

Continuation of the constant humidity test was not possible after 2,000 hours, because the material became brittle due to hydrolysis causing lack of mechanical support to break the structure of the tags [Fay07][Saa10b]. In the humidity cycling test the exposure time for the 85 %RH and 85 °C was significantly shorter and thus no similar effect was observed in that test. However, it is likely that some hydrolysis also occurred in this test.

In the failure analysis of the humidity cycling test, cracks in the wiring of the antenna of the tag were observed near the chip of the tag in test series B and C. However, no similar failure mechanism was observed in most of the test samples from test series A and D. In SEM examination no obvious failure mechanism was observed. Consequently, it is likely that the impedance matching between the antenna and the chip changed due to oxidation of the pads or the conductive particles, or due to degradation of the polymers. According to other reliability studies of ACA joints in humid environments, oxidation and polymer degradation have been found to be reasons for failures [Lai96][Liu98b][Liu07][Mub09][Yim99]. When the bonding parameters of test series A and B were compared, cracks were observed in the tags with the higher bonding pressure. On the other hand, when the bonding parameters of test series C and D were compared, the cracks were observed in the tags with shorter bonding time and thus with lower degree of curing. As the tags from test series D were more reliable than the tags from test series C, a higher degree of curing seems to improve the reliability in this kind of test. When the tags from test series A and C were compared, the tool temperature in the bonding process was higher in the tags from test series C, but the table temperature was lower. Consequently, it is likely that the thermal gradient caused the differences in the behaviour of the samples in the humidity cycling test.

3.5.2 Effect of humidity aging on adhesion of NCF joints

According to previous studies, humidity may degrade polymers and impair the adhesion of polymeric interconnections [Lin06a][Lin06b][Luo05][Teh04][Tur04]. Consequently, in Publications IV and V, adhesion strength tests were used in addition to resistance measurements during constant humidity tests.

In Publication IV, NCF was used to attach test chips to Al_2O_3 substrate. Test chips with gold stud bumps were used. The height of the stud bumps after bonding was approximately 35 µm. Bumps were used without further processing after the bumping process, so no coining was used.

Adhesion strength tests were conducted after every 500 testing hours for seven or eight samples until 2,500 hours. In addition, failures during humidity testing were monitored using the daisy chain resistance of the test samples. The first failure occurred after 2,000 hours and finally seven out of the eight test samples, remaining after 2,000 hours, failed until test was ended after 2,500 hours. The Weibull plot of the results is shown in Figure 17. Scale parameter of the Weibull distribution (η) is 2,333 hours and shape parameter (β) 17.76.

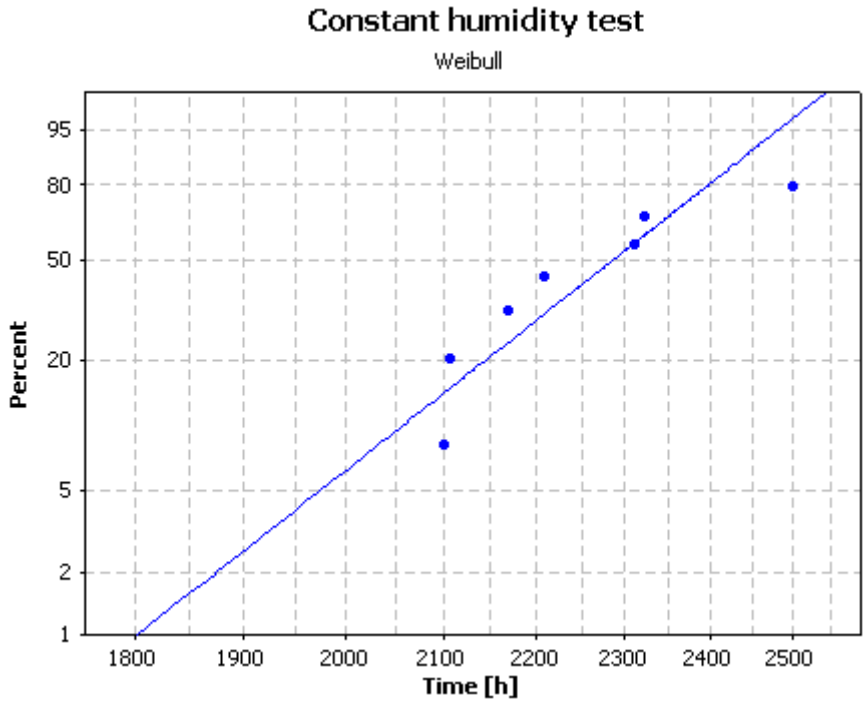

Figure 17: Results of constant humidity test for NCF joints with Al_2O_3 substrate.

In the adhesion strength test the pushing forces needed to separate a test chip from a substrate were measured and converted into congruent shear stresses. The results of the adhesion strength tests are presented in Figure 18. It can be clearly seen that the adhesion deteriorated during the long-term exposure to humid environment. When the test samples became wet at the beginning of the test, the adhesion was significantly impaired. Nevertheless, the deterioration continued after saturation as a function of time, although the decrease in shear strength was slower. After 1,500 hours there were technical problems in the humidity chamber and the chamber was out of order for 590 hours. During that period the samples had time to dry. In consequence the adhesion of the attachments recovered remarkably. Consequently, that measurement point has been excluded from the analysis.

In Publication V, NCF joints were attached onto an FR-4 substrate. Adhesion strength tests were conducted after 500, 2,000 and 4,000 testing hours. Daisy chain resistances were also monitored during testing for detection of failures. A small increase in the resistance was observed, but none of the samples were deemed to have failed during the test. Nevertheless, according to the adhesion strength measurements, it was observed that the adhesion decreased during testing. At the beginning of the test the adhesion decreased markedly, as the test samples became wet. However, with these test samples, too, the deterioration continued after that as a function of time. The results of adhesion strength tests of NCF joints with FR-4 substrate are presented in Figure 19.

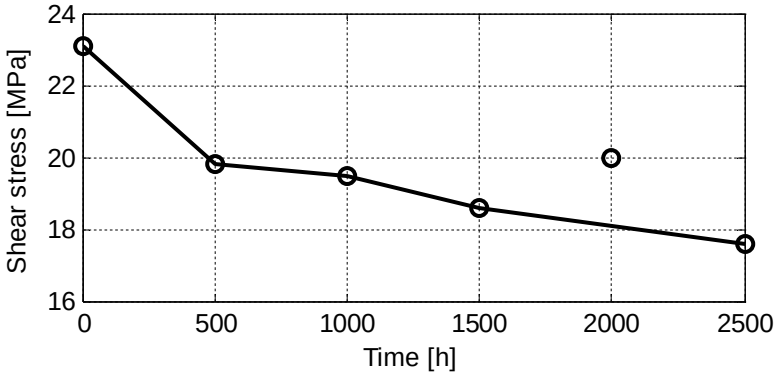

Figure 18: Results of adhesion strength test of NCF joints with Al_2O_3 substrate.

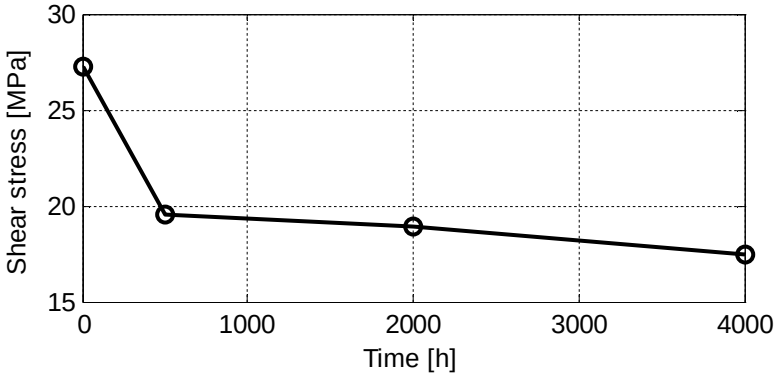

Figure 19: Results of adhesion strength test of NCF joints with FR-4 substrate

Joints of two test samples with FR-4 substrate after each test period were examined using SEM. Most of the joints were flawless and a typical joint can be seen in Figure 20. However, incipient delamination between bump and pad was observed in a few corner joints, but not in most of them. No delamination or cracks in other joints or in other materials and material interfaces were detected. The incipient delamination was occasional. It was already observed in one sample after 500 hours testing. On the other hand, even after 4000 hours testing there were samples without signs of delamination. Figure 21 shows an interface of a pad and a bump with a delamination.

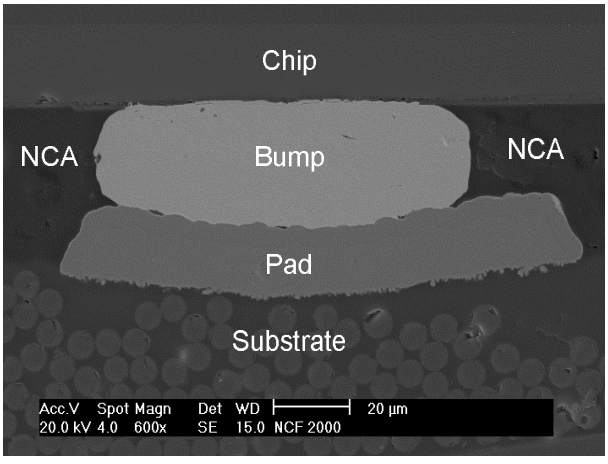

Figure 20: A NCF joint without signs of failure.

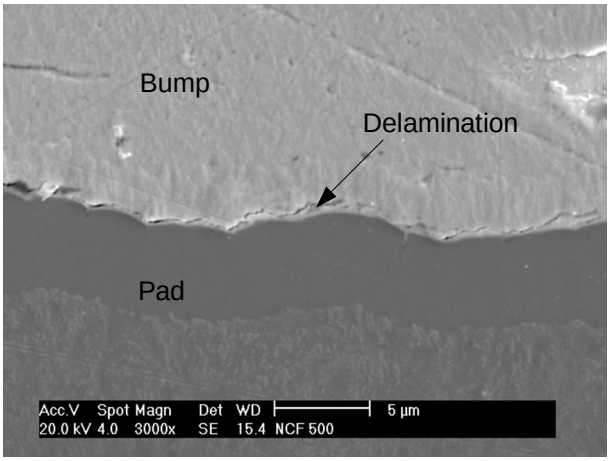

Figure 21: A delamination in the interface of the bump and the pad of a corner joint.

4 Shear stress modelling

Modelling is a powerful tool for the numerical solution of a wide range of engineering problems [Cha02]. Using modelling, time and cost savings can be achieved if the need for prototyping and testing can be reduced [Ada99][Suh02]. Nevertheless, there is lack of effective models describing failures of polymeric interconnections in ALTs [Lin08a] [Liu98b]. Modelling polymer interconnections in ALTs is challenging due to the numerous factors which may affect the materials and material interfaces during testing. Furthermore, the development of good model is challenging, as it should be simple and suitable for new applications or new environments [Suh02].

4.1 Finite element modelling

Finite element method (FEM) is one of the commonly used methods in modelling [Mot96]. In FEM a continuous system is divided into a finite number of smaller parts, called elements [Cha02][Mot96][Zie94]. The elements are connected to each other via shared points, known as nodes [Mot96][Zie94]. In FEM analysis the problem is solved in each element separately. Through the shared nodes, the results of the other elements are taken into account and a solution for the whole system is achieved. [Mot96][Zie94]

In this study FEM was used to model test structures in the test environments. According to previous studies, temperature and humidity seem to be two main factors affecting the reliability of polymeric interconnections [Lah06][Lai96][Lin08b][Yim99][Zho05b]. In thermal and humid environments polymeric materials expand and contract more than metals or ceramics [Lau98b][Teh05][Yin05a][Zho05b]. This mismatch causes stresses on the joints, and when the stresses increase above the endurability of the structure, a failure will occur [Kwo06b][Tum01][Zho05b]. The stresses caused by expansion and contraction due to changes in temperature are called thermo-mechanical stresses [Kwo06b][Yin03]. Conversely, hygro-mechanical stresses arise when materials absorb moisture [Ard03][Won02a][Zho05b].

According to the reliability studies of the ACA joints, shear strength seems to be a major factor in impairing reliability [Kwo06b][Lin08b]. During aging, shear strain may be induced in the joints and the shear strength of the ACA may deteriorate [Lin08b]. As a good predictive model should be simple and suitable for new applications and environments [Suh02], relatively simple shear stress models were used in this study.

Stress and strain models have been used together with experimental testing in earlier reliability studies of polymeric interconnections. In those studies the modelling has been typically used as help in failure analysis to find factors causing failures [Cae03][Mer03] [Par10][Wan09][Yin05a][Yin05b][Zho05c]. In addition, it has been used to understand the effects of environments [Lu10b][Teh05][Tsa06][Tsa08][Yin03] and as an aid in analysing the experimental results [Hua10][Won02a][Yin05a][Zho05c]. Moreover, the modelling has been used in predicting failure mechanisms and places in a test environment [Wei02][Yin06]. Life-time modelling of polymeric interconnections has been found to be challenging, and accurate and useful model to various environments have not yet been achieved [Cae03][Wun08][Wun09]. The aim of this study was to study whether relative simple stress models can be utilised in reliability prediction of polymeric interconnections on the basis of the reliability information obtained from another reliability test.

Modelling consisted of three main steps; building a model, solving it and analysing the results [Ada99]. In the building phase the geometry of the test structure was created. Symmetry was utilised and only one quarter of the test samples were modelled. After that the material properties for the different sections of the geometry were defined. For accurate modelling, accurate material properties are essential and consequently, they were measured in the testing conditions. Next the model was divided into elements using meshing. Refinement was used around the joints to be able to make the models mesh independent. Finally in the building step the boundary conditions were defined. In this study boundary conditions included defining symmetry axis, stress-free conditions and environmental conditions. In the next step the model was solved and in the final step the results were analysed by comparing them to the results of experimental testing. The steps of the modelling process are illustrated in Figure 22.

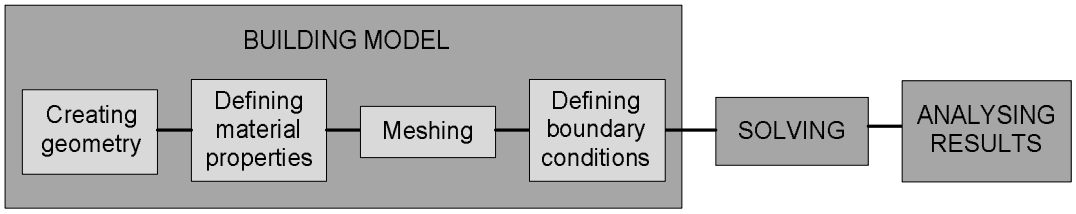

Figure 22: Main steps of modelling [Ada99].

Three different types of models were used in this study. The shear stresses in thermal tests were calculated using thermomechanical modelling. For shear stress simulations of humidity tests hygro-mechanical modelling together with thermomechanical modelling were used. Moreover, diffusion of moisture in the test samples during testing was simulated using a diffusion model. In the diffusion model the wetness of the test samples was solved as a function of time. In the mechanical modelling samples were assumed to be fully saturated and their temperature was assumed to be balanced with the temperature of the ambient environment and therefore stresses were solved in steady state. The modelling was done with finite element based software Ansys. Because the focus was on the polymeric interconnections, only the test structures near the chip were modelled. Three-dimensional models were created.

4.2 Material parameters

For accurate modelling results material properties in the testing environment are required [Ada99][Cae03][Teh04][Teh05][Won02a]. In mechanical modelling Young's modulus (E) and Poisson's ratio, which describe elastic properties of materials, are essential [Ada99][Cha02]. In thermo-mechanical modelling the coefficient of thermal expansion (CTE), which describes the expansion of a material when the temperature changes, is needed in addition to the Young's modulus and the Poisson's ratio [Ada99]. Young's modulus and CTE of polymers change significantly when their glass transition temperatures are exceeded [Har04][Kwo04b][Men08][Men09]. Therefore, the T_g temperatures of the polymers should also be known.

In humidity modelling the coefficient of moisture expansion (CME) and saturated moisture concentration (C_{sat}) need to be defined, in addition to the Young's modulus and Poisson's ratio [Won02a][Won02b]. CME describes the expansion of a material when it absorbs moisture [Fan09][Ma06][Zho05b] and C_{sat} measures the moisture absorption capacity [Fan09][Fan10][Jed08]. When the diffusion of moisture is

modelled, a diffusion coefficient (D) is required in addition to C_{sat} [Jed08][Won02a]. The diffusion coefficient describes how fast a material absorbs moisture [Fan09][Jed08] [Yoo09]. All these parameters are dependent on the temperature and relative humidity of the environment [Fan09][Jed08][Teh05][Wun08]. Therefore for accurate modelling they need to be measured in the testing environment.

4.2.1 Thermal and mechanical parameters

Thermal analysis (TA) is a group of techniques which are used to define connections between temperature and specific properties of materials [Men09]. Thermo-mechanical analysis (TMA) and dynamic mechanical analysis (DMA) are two of these techniques [Kwo06b][Men09] and they were used in this study. TMA is used to measure changes in length or volume under static load as a function of temperature or time [Ehr04] [Men09]. One of its main functions is to measure CTE [Ehr04][Kwo06b][Wun09] [Yeo04]. In addition, it can be used to measure, for example, Young's modulus [Men09].

CTEs of ACFs in Publication VI, and CTEs of ACP and PET substrate in Publications II and III were measured using TMA. The CTEs were determined by measuring changes in the length of the samples as a function of temperature. CTE measurements were made twice for each of the samples, as during the first measurement thermal history was excluded and thermal stresses were evened out [Ehr04][Men09]. The results of the second measurements were used in modelling. For the thermal modelling, the CTEs were calculated on the basis of the results of the TMA measurements using the equation:

$$\alpha = \frac{dl}{dT \cdot l_0} \tag{2}$$

where α is CTE, dl/l_0 is the relative dimensional change and dT is the temperature change [Ehr04][Men09][Tum01]. In order to define the dimensional and temperature changes, a reference point for them was needed; this was chosen to be the stress-free temperature of a model. With each of the stress-free temperatures the reference points were different.

The TMA was also used to measure the Young's modulus of PET substrate and ACP in Publications II and III. Samples were exposed to increasing stress and the resulting strain was monitored. Young's modulus was determined by calculating the slope of the stress-strain curve. Temperature was held constant in each measurement. Therefore, to be able to estimate the Young's modulus as a function of temperature, the measurements were made separately at several temperatures. The measurement temperatures were chosen with intervals of a maximum 20 degrees Celsius. In the temperature range between the measurement points, the Young's modulus was assumed to change linearly.

DMA can also be used to measure the mechanical properties of materials [Ehr04] [Kwo06b][Men09][Yeo04]. In the analysis the sample is exposed either to a small cyclic strain when resultant stress is monitored or to a cyclic stress when the resulting strain is measured [Men09]. From the measurement results storage modulus and loss modulus for the material can be defined [Ehr04][Men09][Yeo04]. Storage modulus describes the elasticity of the material, as also does Young's modulus, which is

measured under a constant load [Ehr04][Men08][Men09]. Consequently, Young's modulus can be approximated to be the same as the storage modulus for elastic materials [Men09]. In Publication VI DMA was used to determine Young's moduli of ACFs as a function of temperature. A cyclic stress with low frequency was applied to the ACF samples as a function of temperature. In the modelling of Publication VI the measured storage moduli were assumed to be the same as the Young's moduli.

T_g temperatures of the polymer materials were also defined on the basis of the TMA and DMA measurements [Kwo04b][Yeo04]. The CTE of polymers increases and Young's modulus decreases significantly when the T_g temperature is exceeded [Ehr04][Har04] [Kwo06b][Men08][Men09]. In Publication VI the T_g temperatures of the ACFs were defined of the results of the DMA and the TMA measurements. In Publications II and III the T_g temperatures of the ACP and PET were defined from the results of CTE measurements.

Poisson's ratio for the adhesives and the PET substrate were estimated on the basis of the literature [Pro11][Spe05][Teh05][Yeu98]. The values of Young's modulus, CTE and T_g temperature of NCF and ACFs used in Publications I, IV and V were from their manufacturer. In addition, the values of Young's modulus, Poisson's ratio and CTE for the chip, the bumps and the pads of every test structures and for the ceramic substrate used in Publication IV were collected from the reference [Mat11]. Moreover, the material parameters and T_g temperature for the FR-4 substrate used in Publications I, V and VI were from its manufacturer.

4.2.2 Moisture parameters

When the relative humidity of the environment of a polymer is increased, the polymer starts to absorb moisture until it reaches its saturation point in that environment. Conversely, desorption of moisture occurs in a polymer when the relative humidity of the environment is decreased. Fick's diffusion law is used to predict the diffusion of moisture in polymer materials [Fan09][Fan10][Zho05b]:

$$\frac{\partial C}{\partial t} = D\left(\frac{\partial^2 C}{\partial x^2} + \frac{\partial^2 C}{\partial y^2} + \frac{\partial^2 C}{\partial z^2}\right) \tag{3}$$

where D is the diffusion coefficient, C is moisture concentration, t is time and x, y and z are the dimensions of a material. Although Fick's law describes the diffusion of most polymers very well, non-Fickian behaviour may need to be taken into account at high temperatures [Fan09]. Notably, epoxy at high temperatures may not completely follow Fick's law. Nevertheless, in this work Fick's law was utilised in the diffusion modelling, in which the aim was to estimate the times for the saturation of the test samples. It was assumed that Fick's law was suitable for this purpose.

The diffusion coefficient describes the diffusion rate of moisture in the material and is needed in diffusion modelling [Fan09][Jed08][Teh05][Won02a][Yoo09]. The diffusion coefficient is heavily dependent on the temperature and relative humidity of the ambient environment [Fan09][Jed08][Teh05]. When a pure material is exposed to an environment with constant temperature and relative humidity and the mass of absorbed moisture is measured as a function of time, the diffusion coefficient in that environment can be determined by fitting the measurement data into an equation which is based on Fick's diffusion law [Jed08][Teh05][Zho05c]:

$$\frac{M_t}{M_{sat}} = 1 - \frac{512}{\pi^6} \sum_{l=0}^{\infty} \sum_{m=0}^{\infty} \sum_{n=0}^{\infty} \frac{\exp(-D \cdot t \cdot L_{eqv})}{(2l+1)^2 (2m+1)^2 (2n+1)^2} \tag{4}$$

where

$$L_{eqv} = \pi^2 \left\{ \left[\frac{(2l+1)^2}{x_0} \right] + \left[\frac{(2m+1)^2}{y_0} \right] + \left[\frac{(2n+1)^2}{z_0} \right] \right\}, \tag{5}$$

M_t is the mass of the absorbed moisture at time t, M_{sat} the saturated mass of moisture, D the diffusion coefficient, and x_0, y_0 and z_0 the dimensions of the sample.

Saturated moisture concentration, C_{sat} is another moisture parameter describing the behaviour of a material in a humid environment. C_{sat} describes the maximum mass of moisture (M_{sat}) which it can absorb per a volume unit (V) [Fan09][Fan10][Jed08] [Yoo09]:

$$C_{sat} = \frac{M_{sat}}{V} \tag{6}$$

It also depends on the temperature and relative humidity of the ambient environment [Fan09][Jed08][Teh05]. However, when the temperature is constant the relation of relative humidity is linear [Fan09][Yoo09].

When materials absorb moisture, they expand [Fan09][Ma06][Teh04][Won02a]. Polymers expand more than metals or ceramics and as a result stress or strain may be induced in the adhesive attachments [Ma06][Won02a]. The amount of expansion can be expressed via hygroscopic strain, ε_h. It is the change in length (Δl) compared to the initial length (l_0) of a polymer as a result of humidity expansion [Ma06]:

$$\varepsilon_h = \frac{\Delta l}{l_0} \tag{7}$$

The coefficient of moisture expansion (CME), which is the material parameter describing the moisture expansion, can be defined on the basis of hygroscopic strain and saturated moisture concentration [Fan09][Fan10][Ma06][Zho05b][Zho05c]:

$$CME = \frac{\varepsilon}{C_{sat}} \tag{8}$$

Like the other two moisture parameters, it is also dependent on the temperature and relative humidity of the environment [Ma06][Teh05][Zho05c].

In this study, moisture modelling was made for the test structures in Publications III, IV and V. For the modelling diffusion coefficients, saturated moisture concentrations and coefficients of moisture expansions for chip material, metals and FR-4 substrate were collected from the reference [Teh05]. The ceramic substrate in Publication IV was assumed to exhibit moisture behaviour similar to that of silicon and metals, and therefore the same moisture parameters from the reference [Teh05] were used for it. In Publications IV and V the moisture parameters of NCF were average values of other

epoxy-based NCA materials from references [Cae04][Teh04][Teh05]. Likewise for the test samples in Publication III, the average values of the moisture parameters of four epoxy-based ACAs from the reference [Teh05] were used for ACP. It was assumed that the average values for the adhesives would describe their behaviour in a humid environment with sufficient accuracy. However, for the PET substrate in Publication III the moisture parameters were measured. A moisture analyser was used in the definition of the diffusion coefficient and saturated moisture concentration when saturated test samples were dried in the analyser and the reduction of their mass was measured as a function of time. Additionally, the coefficient of moisture expansion was calculated from hygroscopic strain which was measured using TMA.

All moisture parameters were defined in an environment with a temperature of 85 °C and a relative humidity of 85 %. This was the environment of the constant humidity test and one extreme condition of the humidity cycling test. To be able to simulate stresses in the other extreme condition of the humidity cycling test, conversion of the moisture parameters to the environment with temperature of 85°C and relative humidity of 10% was needed. As there were no changes in the temperature, it was assumed that the saturated moisture concentration was linearly dependent on the relative humidity [Fan09]. According to measurements in reference [Yoo09], the diffusion coefficient of ACA does not depend on the relative humidity and in addition the relative humidity has only a minor effect on the diffusion coefficient of FR-4. It was therefore concluded that the relative humidity had no influence on the diffusion coefficients of any of the materials used in the Publication V. Additionally, according to the studies by [Yoo09], CMEs of ACA and FR-4 do not seem to depend on the relative humidity if the temperature is constant. Therefore in this study CMEs of the materials were assumed to be the same under both conditions.

4.3 Modelling process

In thermomechanical and hygro-mechanical modelling stresses in steady state under thermal or hygro loads were calculated. Higher stresses were assumed to indicate lower reliability. Thermal modelling was done using a thermal module of the software. The thermal module was also used in humidity modelling via an unambiguous analogy between material parameters [Ard03][Fan10][Ma06][Won02a][Won02b][Zho05b]. The analogy of thermal and moisture parameters is shown in Table 9.

Table 9: Temperature-Wetness analogy [Saa08][Won02a][Won02b].

Properties	Thermal	Moisture
Field variable	Tempereture, T	Wetness, W
Density	ρ	1
Thermal conductivity	k	$D * C_{sat}$
Heat capacity	c	C_{sat}
Coefficient of thermal expansion	α	$CME * C_{sat}$

In finite element modelling displacements of nodes of elements are calculated using matrix calculation. With the help of displacements it was possible to calculate stresses and strains. In thermomechanical and hygro-mechanical modelling stresses are

calculated as a function of material matrix (D), element strain-displacement matrix (B), displacements (q) and thermal or hygro strains (ε_0) [Cha02]:

$$\sigma = D(Bq - \varepsilon_0) \tag{9}$$

In three-dimensional models stress has six components; three normal stresses (σ_x, σ_y, σ_z) and three shear stresses (τ_{xy}, τ_{yz}, τ_{xz}) [Cha02]:

$$\sigma = \left[\sigma_x, \sigma_y, \sigma_z, \tau_{xy}, \tau_{yz}, \tau_{xz}\right]^T \tag{10}$$

Thermal strain also has six components; three normal strains (ε_x, ε_y, ε_z) and three shear strains (γ_{xy}, γ_{yz}, γ_{xz}). Shear strains are zero, but normal strains can be calculated as a function of CTE (α) and temperature change (ΔT) [Cha02][Mer03][Yin05a][Yin06]:

$$\varepsilon_{0thermal} = \left[\varepsilon_x, \varepsilon_y, \varepsilon_z, \gamma_{xy}, \gamma_{yz}, \gamma_{xz}\right]^T = \left[\alpha\Delta T, \alpha\Delta T, \alpha\Delta T, 0, 0, 0\right]^T \tag{11}$$

Hygroscopic strain likewise has six components. Normal hygro-strains can be calculated as a function of CME (β) and moisture concentration (C) [Mer03][Yin05a] [Yin06]:

$$\varepsilon_{0moisture} = \left[\varepsilon_x, \varepsilon_y, \varepsilon_z, \gamma_{xy}, \gamma_{yz}, \gamma_{xz}\right]^T = \left[\beta C, \beta C, \beta C, 0, 0, 0\right]^T \tag{12}$$

The theory and equations behind the modelling are explained in more detail in references [Cha02], [Zie94] and [Mot96].

In the modelling of humidity tests, the effects of moisture and temperature were simulated separately, and to achieve the total effect of the environment they were added together. To obtain total strain in a structure exposed to both changed temperature and changed humidity, thermal strain and hygro strain are added together [Kwo06b][Lah06] [Yin06][Zho05c]. Thermal strain indicates expansion caused by a change in temperature, and hygro strain indicates expansion caused by a change in humidity. As the stresses in the models of this study were elastic, corresponding strain can be defined as a quotient of stress and Young's modulus, and therefore the stresses could also be added together [Yoo09].

To be able to calculate the stresses in the structures, the bumps and pads in the mechanical models were attached to each other making sliding and opening between them impossible. The aim of the modelling was to study the shear stresses in the joints during testing. Before failure the cured adhesive matrix holds the bumps and the pads in contact and greatly restricts movement in the joints [Kri98][Teh04]. As the object of the models was to describe the situation before failure, it was assumed that there would be no movement in the joints before this point.

In thermo-mechanical modelling three different stress-free temperatures were used. One of the temperatures was room temperature of 20°C. The contact stresses in the samples were assumed to be equal at this temperature. In addition, the T_g temperatures of the ACAs and the substrate of the RFID tag were also chosen as stress-free temperatures. It was assumed that above the T_g temperature the Young's modulus of ACA is low enough to reduce the contact stresses forming in the structure. When the temperature falls below the T_g temperature, the ACA changes from a soft form to a hard form and

the contact stresses increase as the ACA shrinks [Kwo04b]. Thus the T_g-point of the adhesive was chosen to be one of the stress-free temperatures. In Publications I, IV and V where ACF and NCF joints were studied, room temperature was used as a stress-free temperature. In Publication VI where joints with two different ACFs were compared, T_g temperatures of the ACFs were chosen as stress-free temperatures. For the thermo-mechanical modelling of ACP joints in Publications II and III all three stress-free temperatures were used and the results were compared. In hygro-mechanical modelling 0%RH was chosen as stress-free humid condition.

When the results were analysed, times for moisture diffusion were calculated and places for highest shear stresses were looked for. Highest shear stresses in all models were observed around corner joints. Consequently, shear stresses around the corner joints as a function of temperature and humidity were simulated. An example of the meshing and of the shear stresses in a quarter of the chip of RFID tag used in Publications II and III is shown in Figure 23. The joint is under the chip, in the upper right corner of the chip. The red areas indicate high positive shear stress values and the blue areas the high negative values. Positive shear stress indicates tensional shear stress and negative compressive shear stress. The absolute values of shear stresses are the lowest in the green areas.

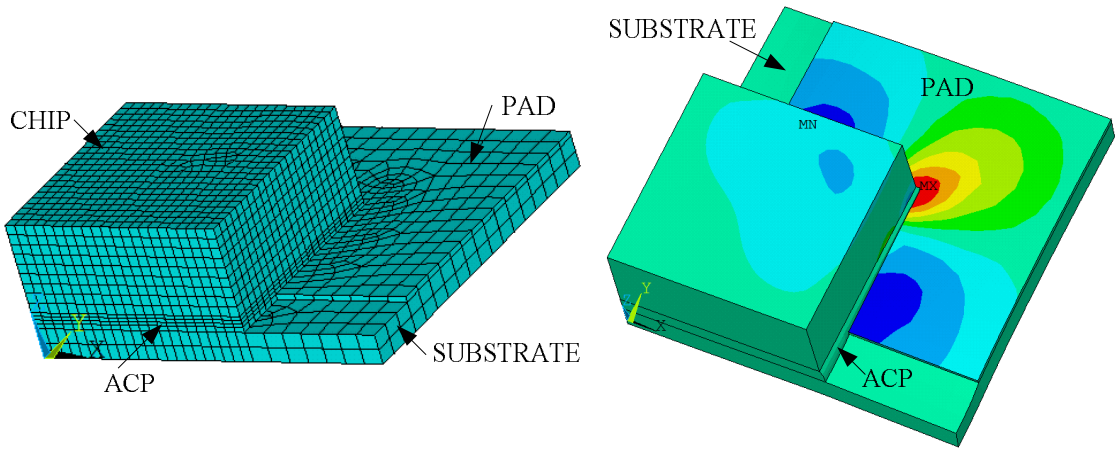

Figure 23: An example of meshing and shear stresses in the joints of the RFID tag.

4.4 Modelling of thermal tests

In this study, the prospects for using relatively simple shear stress modelling in the reliability prediction of polymeric interconnections in thermal tests were examined. Test structure, test materials or thermal tests were varied to see if modelling together with reliability data of another test or from the same test for almost similar test structure could be used in the prediction of reliability so that the need for testing could be reduced. First the materials of a test structure were varied by comparing two different ACF materials in a temperature cycling test. Next the thicknesses of substrate and chip were varied when test samples with the same materials were tested in a temperature cycling test. Finally, test samples with the same materials and structure were tested in different thermal tests. In each case it was investigated if the differences between the test series could be estimated on the basis of modelling. The results of modelling of thermal tests are presented in this chapter.

4.4.1 Comparison of ACF materials

In Publication VI, the prospects for utilising shear stress modelling in the prediction of the reliability of two different ACFs with an organic FR-4 substrate in temperature cycling testing from -40 °C to 125 °C were examined. The shear stresses were calculated at different temperatures from the range of cycling test temperatures using thermomechanical modelling. On the basis of the modelling results, corner joints were assumed to be the most likely places for failures, as the highest values of shear stresses in the adhesive were found to be in their vicinity [Saa09]. In the failure analysis of experimental testing, delamination was found in the corner joints or in the nearby joints. Consequently the model corresponds to the experimental tests from the point of view of the failure place.

The shear stresses of the samples with different ACFs in the inner face of the corner joints were calculated and compared as a function of time. The results are shown in Figure 24. The highest shear stress values with both ACFs were observed at the lowest temperatures. Consequently, according to the modelling, it can be assumed that the failures would more likely occur at lower temperatures than at higher temperatures. In the experimental testing, the failures occurred first at the lower extreme temperature and later also at the higher extreme temperature. Hence the results of modelling and experimental testing also seem to correspond from point of view of the failure mode.

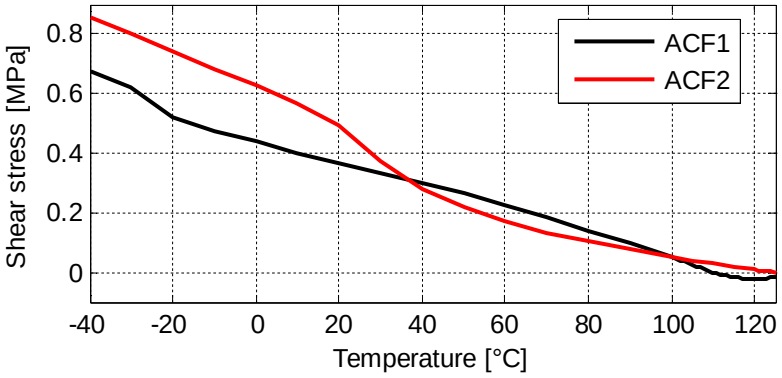

Figure 24: Shear stresses near the corner junction as a function of temperature

In the comparison of test samples with different ACFs the highest shear stresses were observed in the test samples with ACF2. Consequently, on the basis of the modelling, the samples with ACF1 could be assumed to be more reliable than the samples with ACF2. Similar results were also observed in the experimental testing.

The results of the model and the temperature cycling test corresponded. It therefore seems that it may be feasible to use shear stress models to rank these kinds of ACF flip chip joints in order of anticipated failure times in the temperature cycling test. In addition, it seems that shear stress modelling can be used to predict the most likely failure places and failure modes in this kind of test structure during temperature cycling testing.

4.4.2 Comparison of chip and substrate thicknesses

In Publication I shear stresses in test lots with different thicknesses of substrates and chips were modelled in the temperature cycling test from -40 °C to 125 °C. Test lots

with different combinations of ACFs and chip and substrate thicknesses are listed in Table 10. T_g temperature of ACF3 which was used in test lots 1 – 4 was exceeded during testing. This increased its CTE and decreased its Young's modulus significantly. In the model this change was taken into account by changing the material parameters linearly during 20 °C around the T_g temperature.

Table 10: Test lots with different thicknesses of chips and substrates.

	Chip	ACF	Substrate
Test lot 1	480 µm	ACF3	710 µm
Test lot 2	480 µm	ACF3	100 µm
Test lot 3	80 µm	ACF3	710 µm
Test lot 4	480 µm	ACF3	710 µm + RCC
Test lot 5	500 µm	ACF2	600 µm
Test lot 6	500 µm	ACF2	100 µm

The highest shear stresses in each test lot were observed in the inner faces of corner joints. In the failure analysis of the joints after experimental testing, failures were observed in corner joints or joints near them. Consequently, the actual failure places seemed to correspond to the prediction made on the basis of modelling. The shear stresses at the inner face of the corner joint as a function of temperature range of the cycling test were calculated for each test lot. The calculated shear stresses for test lots 1 – 4 are shown in Figure 25 and for test lots 5 and 6 in Figure 26.

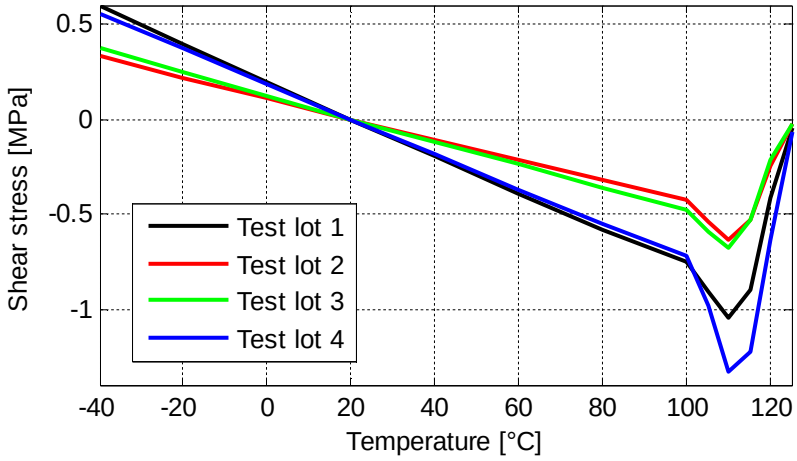

Figure 25: Shear stresses of test lots 1 – 4.

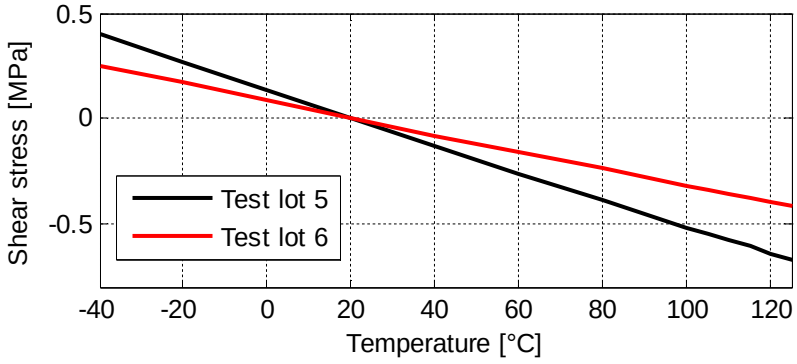

Figure 26: Shear stresses of test lots 5 and 6.

The results show that the thicknesses of the substrate and the chip had an effect on the shear stresses. When the stresses in test lots 1 and 2, and in test lots 5 and 6 were compared, it was seen that the samples with thicker substrates had higher stresses. Similarly the thickness of the chip affected the shear stresses. Due to the thinner chip in test lot 3, it had smaller shear stresses than those in test lot 1. Higher stresses were €assumed to indicate lower reliability. Hence, according to modelling, the samples with thinner chips and substrates are assumed to be more reliable. The results corresponded to the results of experimental testing which showed clearly better reliability with thinner chips and substrates.

The effect of the RCC layer on top of the substrate can be seen by comparing the shear stresses of test lots 1 and 4. Before the T_g temperature of ACF3 these test lots had almost identical shear stresses. However, after the T_g absolute value of the shear stress of test lot 4 was higher. The RCC layer had higher CTE than the FR-4 substrate. Therefore it expanded more as a function of temperature than the chip. This caused higher shear stress on the joints. This behaviour was observed in the temperatures around the glass transition temperature of the ACF3. However, at the lower temperatures the stresses between test lots 1 and 4 were equal. At those temperatures the CTE of ACF3 was smaller than the CTE of the RCC layer. Consequently, the RCC was not able to expand as much it would have without any restrictions from the structure, and shear stress was formed inside the RCC layer instead of ACF3. According to the modelling, the addition of the RCC layer should decrease reliability of the test samples in temperature cycling test, but the difference would be quite small. However, in the experimental testing the results were the opposite, when the addition of the RCC layer improved the reliability significantly. It is possible that these two test lots underwent different failure mechanisms during testing. The cracking of the substrate material observed in the samples of test lot 1 was not observed in any of the samples from test series 4. The absence of these cracks could explain the difference. It is possible that the samples with RCC layer had different contact stresses after bonding than the samples without the RCC. However, as in the modelling these contact stresses were assumed to be equal, the modelling results no longer corresponded to the results of testing.

The highest shear stresses of each test lot were observed at the highest temperatures. Consequently, on the basis of modelling, the samples were assumed to fail at the upper extreme temperature. However, this was heavily dependent on the choice of stress-free temperature. Opposite results were obtained when T_g temperature of the adhesive was chosen as a stress-free temperature. In the experimental studies failure modes were dependent on the bonding pressure. With low bonding pressures, the samples failed at the upper extreme temperature, but with high bonding pressures in the lower extreme temperatures. Consequently, the failure mode cannot be predicted positively on the basis of this kind of modelling. In addition, it was not possible to estimate the effect of bonding pressure on the basis of the modelling.

4.4.3 Comparison of thermal tests

In Publication II RFID tags were tested in two temperature cycling tests with temperature ranges of -40 °C to 125 °C and -40 °C to 85 °C, and in two constant temperature tests with temperatures of 125 °C and 85 °C. Prospects for using shear stress modelling in the reliability prediction of ACA joints in different thermal tests were examined using the test structures and reliability results of experimental testing of Publication II as a reference.

The highest shear stresses in the ACP were seen around the joints. The shear stresses in the inner face of a joint were calculated at different temperatures from -40°C to 125°C, which is the temperature range of the wider temperature cycling test. In addition, it includes the temperature range of the other temperature cycling test as well as the temperatures of the constant temperature tests. The results with three different stress-free temperatures are presented in Figure 27.

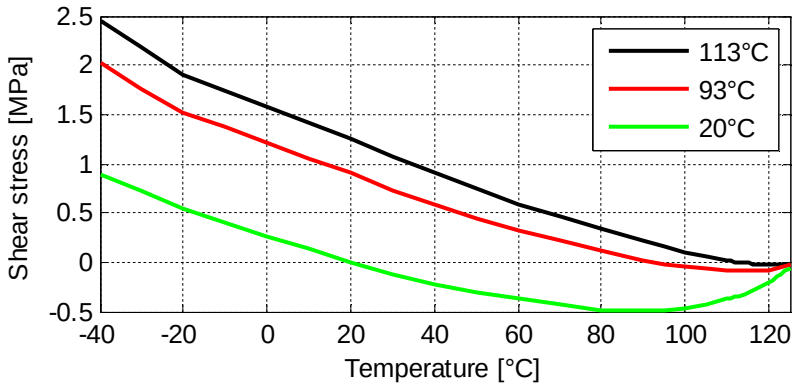

Figure 27: Shear stress with different stress-free temperatures as a function of temperature.

According to the modelling the temperature cycling tests seemed to be more demanding than the constant temperature tests. The temperature cycling tests created higher shear stresses and in addition, the stresses in the cycling tests were fluctuating which may increase harshness even further. Consequently, according to the modelling failures can be assumed to occur faster in the cycling tests. Such behaviour was also observed in the experimental testing.

When the shear stresses in the temperature ranges of the cycling tests were compared, the highest stresses were equal and there was only a small difference in the fluctuating range of the stresses between the tests. Thereby, according to the modelling, it was assumed that the test samples in the -40 °C to 125 °C test might fail slightly faster than the test samples in the -40 °C to 85 °C test. Additionally, it could be assumed that the differences in the failure times would not be remarkable. However, this was contrary to the experimental tests, where a significant difference in the failure times was observed. Moreover, in the temperature cycling test from -40 °C to 125 °C significant differences in failure times of test samples with different bonding parameters were observed, samples with higher bonding temperature being significantly more reliable than the others. Nevertheless, it was not possible to predict these differences on the basis of the modelling, as it was not possible to take into account the effects of bonding parameters in the simple shear stress modelling.

Failure modes estimated on the basis of modelling did not correspond to the results of experimental testing either. The highest shear stresses in both temperature cycling tests occurred at the lower extreme temperature and thus the samples were assumed to fail at the lower extreme temperature. However, in the experimental testing samples failed commonly at higher extreme temperature.

As shear stress modelling and the results of experimental testing did not correspond, this kind of modelling is not feasible in the reliability predictions of ACA joints in

different thermal tests. The model gives information about the rigorousness of a test and thereby a prediction of which test will first cause failures is possible. However, the failure times cannot be estimated on the basis of the failure times of the other tests. In addition, this indicates that the failure mechanism in the higher temperature cycling test is not significantly related to shear stress and the model needs to be improved.

Typically, in the bonding process of ACA joints a thin ACA layer is left in the joints between a bump and a pad. Hence, the model was improved by adding a thin ACP layer to the model which made the model more accurate and allowed both sliding and expansion between the bump and the pad. In addition to shear, normal stress and strain of the adhesive layer in the joint has been found to be an important factor to maintain electrical connection [Kwo06b][Wan09]. The expansion is especially important as the ACP used in the test samples had rigid nickel particles which cannot compensate for the expansion of the ACP matrix [Yim98][Yin03][Yin05a]. Due to the expansion of the ACP matrix, the thickness of the ACP layer increases and reduces the contact area between conductive particles and bumps or pads [Kwo06b][Yin03][Yin05a]. As a result, the contact resistance increases [Kwo06b][Wan09][Yin03]. In the experimental testing the resistances increased during the temperature cycling tests, but recovered after testing. Consequently, it is possible that the thin ACP layer in the joint expanded when the temperature increased during testing. To take this expansion into consideration, normal strain in the z-direction was modelled with the modified model. Using the improved model it was possible to take into account the effects of different bonding pressures by varying the thickness of the ACA layer in the model. In the samples from test series B, the layer was measured to be approximately 0.2µm while in the other samples with lower bonding pressure the thickness was approximately 0.3µm. The changes in the thickness of the ACP layer as a function of temperature were calculated with stress-free temperature of 20 °C and the results are shown in Figure 28.

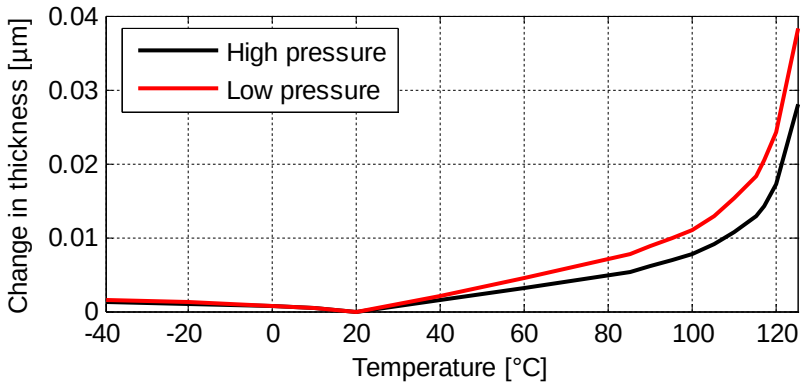

Figure 28: Change in thickness of an ACP layer between bump and pad as a function of temperature with two different bonding pressures.

According to the results of the new model, it is likely that the samples would fail significantly faster in the temperature cycling test of -40 °C to 125 °C than in the -40 °C to 85 °C test. In addition, at a temperature of 125 °C samples with higher bonding pressure seem to be more reliable than the samples with lower bonding pressure. In the temperature range of -40 °C to 85 °C the difference between the samples with different bonding pressures is significantly smaller and the difference in the failure times between the samples with different bonding pressures can be assumed to be small. Moreover, on the basis of modelling the failures would be estimated to occur at the

higher extreme temperature. However, the difference between the extreme temperatures in the -40 °C to 85 °C test is not so significant, and thus it is possible that the samples fail at both extreme temperatures simultaneously. All these predictions made on the basis of the modelling corresponded to the experimental results. No difference between test samples with different bonding pressures were observed in -40 °C to 85 °C testing, but according to the modelling the difference is so small that it may not be noticeable because of natural divergence between test samples.

The modelling of the changes in the thickness of the ACA layers in the joints seems to fit well with the results of the experimental testing. Although estimation of exact failure times was not possible on the basis of the model by comparing to the results of another thermal test, the magnitude of the times could be well predicted. In addition, the modelling corresponded to the assumed failure mechanism and the failure modes seem to fit well with the experimental data. Moreover, the differences between the bonding pressures observed in the experimental testing could be estimated on the basis of such modelling.

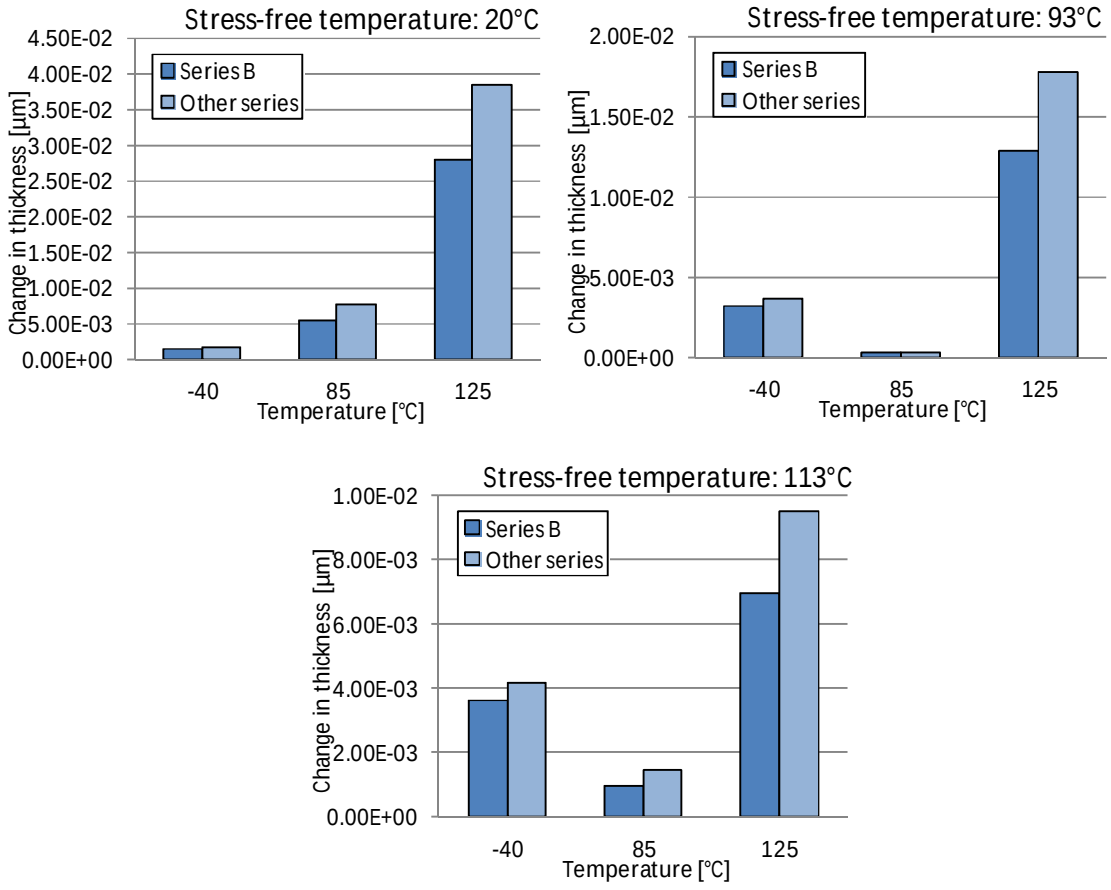

Figure 29: Changes in the thicknesses of ACA layer at extreme temperatures of temperature cycling tests with three different bonding pressures.

Such modelling was done with each of the three stress-free temperatures. The changes in the thickness of ACA layer at extreme temperatures of the tests with each stress-free temperature are shown in Figure 29. Similar types of results were achieved with each stress-free temperature. However, differences in the failure modes were observed. With the other two stress-free temperatures, the samples in the -40 °C to 85 °C test would

have failed according to modelling most probably first in the lower extreme temperature. However, no such behaviour was detected in the experimental testing and thus the model with stress-free temperature of 20°C seems to fit to the experimental data best.

4.5 Modelling of humidity tests

The prospects for using relatively simple shear stress modelling in the reliability prediction of polymeric interconnections under humidity tests were examined using two different methods. As in the thermal tests, the test samples were tested in different humidity tests and the prospects for using modelling together with reliability data obtained from another test were investigated. In addition, the potential to predict failure times on the basis of modelling and shear strength measurements was also examined. The results of the modelling of humidity tests are presented in this chapter.

4.5.1 Comparison of humidity tests

In Publication III RFID tags were tested in two different humidity tests. A constant humidity test with temperature of 85 °C and relative humidity of 85 %, and a humidity cycling test with extreme conditions of 85 °C / 10 %RH and 85 °C / 85 %RH were used. In this study the prospects for using shear stress modelling in the reliability prediction of ACA joints in different humidity tests were examined.

A diffusion model was used to calculate the times to full saturation of the test samples in different test conditions. According to the modelling, it took 69 minutes until the dry test samples were saturated exposed to the test conditions of 85 °C and 85 %RH. Consequently, the test samples in the humidity cycling test saturated during the 2 hours' exposure time at extreme conditions of 85 °C and 85 %RH. In addition, at the extreme condition of 85 °C and 10 %RH the samples dried so that the wetness corresponded to the saturated state of that environment. Consequently, in the hygro-mechanical modelling, shear stresses in the test structure were modelled in the saturated states.

Shear stresses induced by moisture and temperature were modelled with hygro-mechanical and thermo-mechanical models and added together. The highest shear stresses were found to be around the joints at the height of the interface between the pad and the bump. Consequently, it is likely that failures will occur in this interface and the failure mechanism could be in the form of partial opening of the joint or delamination. However, in the failure analysis of the tested samples no obvious failure mechanism in the joints was observed even though the cross-sections of the joints had been examined.

The absolute values of total shear stresses in the ACP on the inner face of the joints at the height of the interface between the pad and the bump are shown in Figure 30. The stresses in both extreme conditions of the humidity cycling test are presented with the three stress-free temperatures. According to the results, selection of the stress-free temperature seems to play an important role. With the two lower stress-free temperatures, it seems that the constant humidity test is a more rigorous test of the samples. Alternatively, according to the results with highest stress-free temperature, there does not seem to be any significant difference.

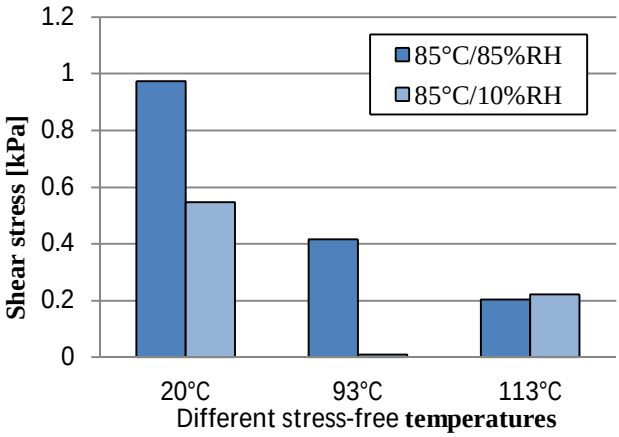

Figure 30: Total shear stresses in extreme conditions of humidity cycling test with three stress-free temperatures.

In addition to the fluctuation of the humidity level, the humidity cycling test also involves decrease in the temperature. The thermal stress as a function of temperature is illustrated in Figure 31. With the two higher stress-free temperatures the thermal stress increased when the temperature decreased and thus the temperature drop in the humidity cycling test appeared to increase the rigorousness of the test. On the other hand, with the lowest stress-free temperature, the drop in the temperature appeared to lower the stress and thus reduced the rigorousness of the test.

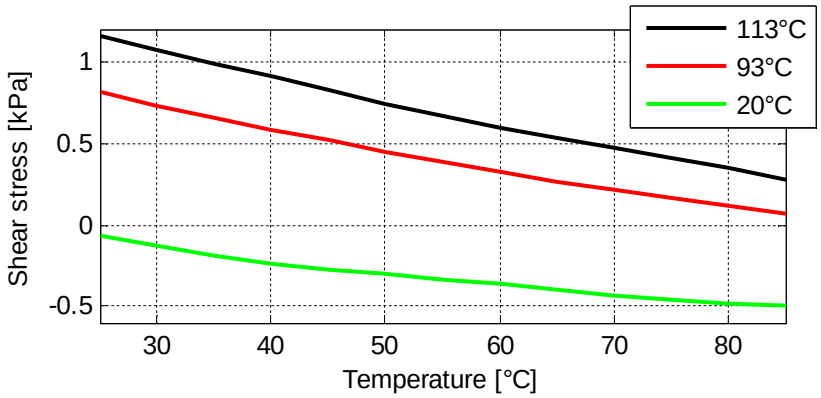

Figure 31: Thermal shear stress as a function of temperature.

When the effect of changing temperature in the humidity cycling test was also taken into account, with the stress-free temperature of 20°C, the humidity cycling test seemed to be a less severe test than the constant humidity test. However, with a stress-free temperature of 113°C, the humidity cycling test seemed to be more severe than the constant humidity test. With a stress-free temperature of 93°C, it was hard to determine the order of the humidity tests. In this case the shear stress decreased significantly when the humidity decreased. However, the shear stress increased even more when the temperature decreased. According to the results of the experimental tests, the samples from test series B and C failed significantly faster in the humidity cycling test than in the constant humidity test. However, the failure mechanism in these samples was not observed on the ACP joints. The samples from the other two test series failed at approximately the same time in both tests. Thus the results of modelling with a stress-

free temperature of 93°C seemed to be closest to the results of experimental testing. However, as the failure in the humidity cycling test for test series B and C occurred in the antennas of the tags instead of in the ACP joints, this kind of modelling of the ACP joints does not describe the actual failure mechanisms. In addition, with this kind of modelling it is not possible to determine the differences in the reliability of the tags with different bonding parameters.

Failures in humid environments may be caused by different factors such as expansion, cracking, oxidation of metal surfaces, degradation of the polymer matrix, loss of adhesion and cohesion, chemical reactions between water molecules and materials, and relaxation [Fan09][Liu11][Mub09][Teh04][Won02a][Wun09][Yin05b]. Consequently, it is likely that failure mechanisms of polymeric interconnections in humidity tests are not only related to stresses and this kind of modelling may be useless for reliability prediction in humid environments.

4.5.2 Effects of humidity aging on adhesion of NCF joints

In Publications IV and V flip chip joints with NCF were tested in a constant humidity test with temperature of 85 °C and relative humidity of 85 %. Two different substrate materials were used; FR-4 and Al_2O_3. The prospects for predicting failure times in a constant humid environment on the basis of shear strength measurements and modelling were examined. Shear strength measurements were made after periods in the constant humidity test to measure changes in contact stresses of the joints during the testing. It was observed that absorption of humidity impaired the adhesion of the joints significantly with both substrate materials. Moreover, the decline of adhesion continued as a function of time in the humid environment. When the contact stresses in the joint weaken enough, the joint will open and fail. At this point the hygroscopic stresses, which are constant during the whole humidity test, exceed the contact stresses holding the bumps and pads in contact. Using modelling the failure limits, under which the adhesion should decrease until a failure occurs were calculated. When the results of experimental testing and modelling were combined, estimation of failure times was possible.

A diffusion model was used to calculate times to full saturation of the test samples with both substrates. With the ceramic substrate it took 560 hours until the structure was saturated and with FR-4 substrate 86 hours. As the constant humidity test lasted for 2,500 hours with the samples with ceramic substrate and 4,000 hours with the samples with FR-4 substrate, all samples became saturated at the beginnings of the tests. Consequently, the stresses in test structures were modelled in the saturated state.

Thermo-mechanical and hygro-mechanical shear stress models were used to model the effects of mismatches in thermal and humid expansions. The stresses were added together and the highest shear stress value was chosen as failure limit. This indicates the stress limit under which the contact stresses must fall for a failure to occur. For the test samples with ceramic substrate the failure limit was 18.1 MPa and for the test structures with FR-4 substrate 11.7 MPa. In the adhesion measurements average contact stresses on the area of the chip were measured. It was assumed that the adhesion of the adhesive to the substrate and to the chip is quite constant as a function of place. Therefore the stresses calculated on the basis of adhesion measurements were compared to the failure limit to be able to estimate magnitude of failure time.

Contact stresses of the test samples with ceramic substrate exceeded its failure limit during the 2,500 hours testing. Therefore, the estimation of the failure time was possible on the basis of modelling. The degradation of contact stress values measured by shear strength measurements and the failure limit defined on the basis of modelling are shown in Figure 32 as a function of time. The measurement point of 2,000 hours differed from the other measurement points because of technical problems and the curve without that point is plotted in the Figure 32. When the measurement point of 2,000 hours is ignored, the failure limit is exceeded at the time point of 2,045 hours. Consequently the magnitude of the failure time of the test samples with ceramic substrate in the constant humidity test was estimated to be around 2,045 hours. In the experimental testing the characteristic lifetime for the test samples was 2,333 hours, which is relatively close to the estimated failure time. According to this study it therefore seems possible to estimate the magnitude of failure time for this kind of test structure in a constant humidity test by using information of shear strength test and modelling.

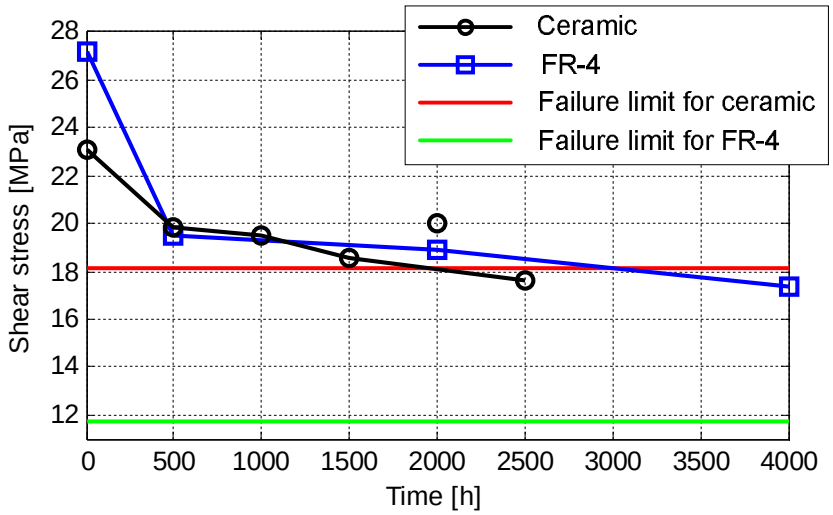

Figure 32: Deterioration of contact shear stresses and failure limits for the samples with different substrates.

The failure limit of the test samples with FR-4 substrate was not exceeded during the 4,000 hours test. The changes in contact stress during testing and the failure limit are also presented in Figure 32. As the failure limit was not exceeded, according to the modelling, it was assumed that no failure would occur during testing. No failures were detected in the experimental testing either, therefore the results of modelling correspond to the results of experimental testing. When the test samples saturated at the beginning of the test, the drop in contact shear stress was fast, but after that it slowed down substantially. After saturation the decline of the contact stress seemed to be relatively linear. With the linear decrease of the contact stress, it would take 13,500 hours until the test samples with FR-4 substrate would exceed their failure limit. Consequently, the test samples with the thin FR-4 substrate appear to be extremely reliable in this kind on humid environment.

The place with the highest shear stress was assumed to be the most likely place for failures. Consequently, according to the modelling, the corner joints were assumed to be the most likely places for failures. In the failure analysis of the test samples with FR-4 substrate, signs of delamination were observed in a few corner joints. However, no

signs of failures were observed in any other joints. Consequently, the failure place estimated on the basis of modelling seems to correspond to the results of experimental testing.

5 Conclusions and final remarks

Polymeric interconnections are an alternative to conventional solder joints with underfills. Because of their advantages polymeric interconnections can be used in numerous applications, and therefore in numerous environments. Nevertheless, reliability problems may occur, especially in demanding conditions. Accelerated life tests are typically used when reliability is studied, but they are typically time-consuming. Utilisation of modelling would decrease the need for testing, and cost and time savings could be achieved. This study explored the prospects for using modelling in the prediction of reliability of ACA and NCA flip chip joints in humid and thermal environments. The aim was to ascertain if shear stress modelling together with reliability data of a test with one type of test structure could be used in the prediction of reliability of slightly changed test structures or different test methods.

It was observed that prediction of reliability in a humid environment is extremely difficult due to numerous factors which may cause failures in humid environments. The failures in humid environments are not related only to stresses; polymer degradation, relaxation, effects of material interfaces and chemical reactions such as oxidation may also impair the electrical properties of the joints as well as the change properties of the materials. In this work, one type of test structure was tested in two different humidity tests and the results between them were compared. Shear stress modelling was used to predict the changes between the tests, and finally the modelling results were compared to the results of experimental testing. The results of modelling were strongly related to the selection of stress-free temperature. In addition, it was not possible to estimate failure mechanisms and places on the basis of the modelling. Consequently it was found that shear stress modelling alone is not suitable for comparison between different humidity tests. However, when NCF flip chip joints were tested in a constant humidity test and the decrease of adhesion in the humid environment was taken into account, failure time estimation in a constant humidity test became possible.

In addition, it was observed that it is important to take failure mechanisms into account in modelling. If shear stress modelling is used, the failure mechanisms should be related to shear stresses. The shear stress modelling was found to correspond to the experimental tests fairly well when the material of ACA was changed or when the thicknesses of the chip or substrate were changed in thermal testing. In the failure analysis of these test samples signs of delamination were found, thus indicating a shear stress related failure mechanism [Luo05]. It therefore appears that this kind of modelling can be used in reliability prediction when only materials or material thicknesses are changed and when the reliability data of the first test structure in the same thermal test is available. Although the shear stress modelling seemed to be useful in the reliability prediction of slightly changed test structure, it was no longer functional when test structure was changed by adding a RCC layer on top of the substrate. The addition of an RCC layer changed the failure mechanism and the shear stress modelling no longer described the factors causing the failures. In addition, when the thermal tests were varied, shear stress modelling was found to give an incorrect result, as it underestimated the differences in reliability between the temperature cycling tests. The failure mechanism of these test samples was assumed to be caused by expansion of the adhesive matrix and not to be related to shear stress. Nevertheless, a strain model which calculated the change in thickness of an adhesive layer between a bump and a pad

during testing corresponded to the experimental result fairly well as it was related to the assumed failure mechanism.

Although the relative simple shear stress modelling seemed to be useful for the estimation of failure time, mode, mechanism and place for some applications, the calculation of accurate failure times was not possible for most of them. To obtain more accurate results, the modelling needs to be improved. In this study it was observed that material properties may change significantly during testing. Consequently, changes in material parameters during testing need to measured and utilised in the modelling. In addition, the visco-elastic behaviour of the materials needs to be taken into account. In this study the material behaviour was assumed to be purely elastic to ensure the simplicity of the models. However, as the failures occur as a function of time viscous characteristics may also be significant. Moreover, the effects of bonding parameters on the contact stresses and their material properties should also be estimated. In this study test samples with different bonding parameters were tested and it was observed that the bonding parameters had significant effects on reliability in the experimental tests. However, it was not possible to estimate the differences between the test samples with different bonding parameters using modelling. By modelling the bonding process, contact stresses could be calculated and possible differences in them with different bonding parameters could be discovered. Furthermore, if accurate life-time estimations without reliability data of another test structure or another test are desired, long-term failure mechanisms such as fatigue, creep and relaxation of an adhesive should also be taken into account in the modelling.

The following paragraphs summarise the main results of the publications.

Publication I, “Reliability of ACF interconnections on FR-4 substrates”, studied the effects of different thicknesses of chips and substrates on the reliability of ACF flip chip joints. Six test lots with two different ACFs, four different substrates and three different test chips were tested in a temperature cycling test. Shear stress modelling was used to study the differences between the test lots in a temperature cycling tests. The results of the modelling and the reliability tests were compared. When only the thicknesses of the substrate and chip were changed their effects on the reliability could be estimated on the basis of modelling. Consequently, shear stress modelling seems to be feasible in the reliability prediction of ACF joints when dimensions of test samples are changed. However, when an RCC layer was added on top of the substrate modelling the experimental results were the opposite. The test samples with the RCC layer had a different failure mechanism, which may explain the discrepancy between the results.

Publication II, “The Effects of Temperature Profile of Accelerated Temperature Cycling Tests on the Reliability of ACA Joints in RFID Tags”, studied the reliability of ACP joints of RFID tags using two constant temperature tests and two temperature cycling tests. The temperature cycling tests were observed to be more usable than the constant temperature tests. In the temperature cycling tests different failure times and modes were observed. In addition, tags with different bonding pressures behaved differently in the temperature cycling tests. In failure analysis no clear failure mechanism was perceived. After both tests resistances of most of the test samples recovered. Consequently, failures were assumed to be caused by mismatch of expansions between polymer matrix and conductive particles of the ACP in the joints. The mismatch caused

degradation of electrical contact during testing but it recovered after testing when the elastic expansion recovered.

Publication III, “Effects of cycling humidity on the performance of RFID tags with ACA joints”, concentrated on the reliability of RFID tags in two different humidity tests. The tags were tested using a constant humidity test and a humidity cycling test. Different failure times, modes and mechanisms were observed in these tests. Failure times in the humidity cycling tests were significantly shorter than the failure times in the constant humidity test. In the constant humidity test most of the test samples failed due to hydrolysis, when the substrate material became brittle and the tags crumbled. In the humidity cycling test the failure mechanism was dependent on the bonding parameters. In two test series cracks in the antennas of the tags, which broke the electrical connection between chip and antenna, were observed. However, in the other two series no obvious failure mechanism was observed.

Publication IV, “Moisture Effects on Adhesion of Non-Conductive Adhesive Attachments”, studied the prospects for estimating the failure times of flip chip joints with NCF and ceramic substrate in a constant humidity test on the basis of modelling and adhesion tests. Experimental testing and adhesion measurements were made. Adhesion was observed to decrease as a function of time during which the samples were exposed to the humid environment. On the basis of modelling the failure limit under which the adhesion should decrease a failure to occur was calculated. When the results of the adhesion tests and modelling were combined, the failure time for the test samples was predicted. When the predicted failure time was compared to the results of testing, it was observed that the results were nearly the same.

Publication V, “Changes in Adhesion of Non-Conductive Adhesive Attachments during Humidity Test”, dealt with flip chip joints with NCF and FR-4 substrate in a constant humidity test. Experimental testing, adhesion measurements and modelling were performed. With this test structure, too, adhesion was observed to decrease as a function of time in the humid environment. According to the modelling the failure limit was calculated and on the basis of adhesion measurements, failure time was predicted. The predicted failure time was not exceeded during testing, nor were any failures detected in the experimental testing.

Publication VI, “Shear stress modelling of ACA joints during temperature cycling testing”, concentrated on the reliability of flip chip joints with two different ACFs in a temperature cycling test. In addition, the prospects for using shear stress modelling in the prediction of the reliability of ACF joints when one ACF is replaced by another, was studied. Using modelling differences in the reliability of the joints with different ACFs were estimated and the result compared to those of the experimental data. The results of modelling and testing were observed to correspond. On the basis of shear stress modelling ACF flip chip joints could be ranked in order of anticipated failure times and likely places for failures could be estimated.

REFERENCES

[Ada99] Adams, V. and Askenazi, A. “Building Better Products with Finite Element Analysis”, OnWord Press, United States of America, 1999, 587p.

[An07] An, B., Cai, X., Chu, H., Lai, X., Wu, F. and Wu, Y. “Flex Reliability of RFID Inlays Assembled by Anisotropic Conductive Adhesive”, Proceedings of HDP'07, Shanghai, China, June 26-28, 2007, pp. 60-63.

[Ard03] Ardebili, H., Wong, E.H. and Pecht, M. “Hygroscopic Swelling and Sorption Characteristics of Epoxy Molding Compounds Used in Electronic Packaging”, IEEE Transactions on Components and Packaging Technologies, Vol. 26, No. 1, 2003, pp. 206-214.

[Ast06] Asthana, R., Kumar, A. and Dahotre, N. “Materials Science in Manufacturing”, Elsevier Inc., United States of America, 2006, 628p.

[Bro99] Brown, W.D. “Advanced Electronic Packaging – With Emphasis on Multichip Modules”, IEEE Press, New York, 1999, 791p.

[Cae03] Caers, J.F.J.M. and Zhao, X.J. “Prediction of Moisture Induced Failures in Flip Chip on Flex Interconnections with Non-conductive Adhesives”, IEEE, Electronic Components and Technology Conference, New Orleans, Louisiana, USA, May27-30, 2003, pp. 1176-1180.

[Cae04] Caers, L.F.J.M., Zhao, X.J., Hansen Sy, G., Wong, E.H. and Mhaisalkar, S.G. “Towards a Predictive Behaviour of Non-conductive Adhesive Interconnects in Moisture Environment”, IEEE, Electronic Components and Technology Conference, Las Vegas, USA, June 1-4, 2004, pp. 106-112.

[Cai08] Cai, X., An, B., Wu, Y., Wu, F. and Lai, X. “Research on the Contact resistance and Reliability of Flexible RFID Tag Inlays Packaged by Anisotropic Conductive Paste", 9th International Conference on Electronic Packaging Technology & High Density Packaging (ICEPT-HDP'08), Shanghai, China, July 28-31, 2008, pp.129-133.

[Cha00] Chan, Y., Hung, K., Tang, C. and Wu, C. “Degradation Mechanisms of Anisotropic Conductive Adhesive Joints for Flip Chip on Flex applications”, Proceedings of 4th IEEE Conference on Adhesive Joining and Coating Technology in Electronics Manufacturing, Espoo, Finland, June 18-21, 2000, pp. 141-146.

[Cha02] Chandrupatla, T.R. and Belegundu, A.D. “Introduction to Finite Elements in Engineering”, 3rd edition, Prentice-Hall, Inc., United Sates of America, 2002, 453p.

[Cha03] Chan, Y.C., Uddin, M.A., Alam, M.O. and Chan, H.P. “Curing kinetics of Anisotropic Conductive Adhesive Film”, Journal of Electronic Materials, Vol. 32, No. 3, 2003, pp. 131-136.

[Che06] Chen, X., Zhang, J., Jiao, C. and Liu, Y. “Effects of different bonding parameters on the electrical performance and peeling strengths of ACF interconnection”, Microelectronics reliability, Vol. 46, No. 5-6, 2006, pp. 774-785.

[Chi01] Chiriac, V.A. and Lee, T.T. “Transient Thermal Analysis of an ACF Package Assembly Process”, IEEE Transactions on Components and Packaging Technologies, Vol. 24, No. 4, 2001, pp. 673-681.

[Dob07] Dobkin, D. “The RF in RFID - Passive UHF RFID in Practice”, WJ Communications, San Jose, 2007, 504p.

[Dom07] Domdouzis, K., Kumar, B. and Anumba, C. “Radio-Frequency Identification (RFID) applications: A brief introduction”, Advanced Engineering Informatics, Vol. 21, No. 4, 2007, pp. 350-355.

[Ehr04] Ehrenstein, G.W., Riedel, G. and Trawiel, P. “Thermal Analysis of Plastics – Theory and Practice”, Carl Hanser Verlag, Munich, Germany, 2004, 368p.

[Fan09] Fan, X.J., Lee, S.W.R. and Han, Q. “Experimental investigations and model study of moisture behaviors in polymeric materials”, Microelectronics Reliability, Vol. 49, No. 8, 2009, pp. 861-871.

[Fan10] Fan, X.J. and Suhir, E. “Moisture Sensitivity of Plastic Packages of IC Devices”, Springer, United States of America, 2010, 570p.

[Fay07] Fayolle, B., Colin, X., Audouin, L. and Verdu, J. “Mechanism of degradation induced embrittlement in polyethylene”, Polymer Degradation and Stability, Vol. 92, No. 2, 2007, pp. 231-238.

[Fri06a] Frisk, L. and Kokko, K. “The Effects of Chip and Substrate Thickness on the Reliability of ACA Bonded Flip Chip Joints”, Soldering and Surface Mount Technology, Vol. 18, No. 4, 2006, pp. 28-37.

[Fri06b] Frisk, L. and Cumini, A. “Reliability of ACA bonded flip chip joints on LCP and PI substrates”, Soldering Surface Mount Technology, Vol. 18, No. 4, 2006, pp. 12-20.

[Fri07a] Frisk, L. and Kokko, K. “Effect of RCC on the Reliability of Adhesive Flip Chip Joints”, Journal of Electronic Packaging, Vol. 129, No. 3, 2007, pp. 260-265.

[Fri07b] Frisk, L. and Cumini, A. “Reliability of ACA Bonded Flip Chip Joints on LCP and FR-4 Substrates”, Proceedings of the 17th European Microelectronics and Packaging Conference & Exhibition (EMPC), Oulu, Finland, June 17-20, 2007, pp. 478-483.

[Fri09] Frisk, L. and Cumini, A. “Effect of Substrate Material and Thickness on Reliability of ACA Bonded Flip Chip Joints”, Soldering and Surface Mount Technology, Vol. 21, No. 3, 2009, pp. 15–23.

[Har04] Harper, C.A. “Electronic Materials and Processes Handbook”, 3rd edition, McGraw-Hill, United States of America, 2004, 800p.

[Hua10] Huang, Y. and Lu, S. “Development and Reliability of Ultra-Thin Chip on Plastic Bonding for Flexible Liquid Crystal Displays”, IEEE, Electronic Components and Technology Conference, Las Vegas, NV, USA, June 1-4, 2010, pp. 575-580.

[Hwa09] Hwang, J., Kim, J., Kang, S., Seo, D. and Kwon, Y. “Feasibility study of non-conductive film (NCF) for plasma display panel (PDP) application”, Microelectronics Reliability, Vol. 49, No. 7, 2009, pp. 806-812.

[Jed08] Jedec Solid State Technology Association, “JEDEC Standard – Test Method fot the Measurement of Moisture Diffusivity and Water Solubility in Organic Materials Used in Electronic Devices - JESD22-A120A”, United States of America, 2008, 8p.

[Jed09a] Jedec Solid State Technology Association, “JEDEC Standard – Steady State Temperature Humidity Bias Life Test – EIA/JESD22-A101-C”, United States of America, 2009, 6p..

[Jed09b] Jedec Solid State Technology Association, “JEDEC Standard – Temperature Cycling – JESD22-A104D”, United States of America, 2009, 12p.

[Jen95] Jensen, F. “Electronic Component Reliability – Fundamentals, Modelling, Evaluation, and Assurance”, John Wiley & Sons Ltd., England, 1995, 355p.

[Kim08a] Kim, J., Kim, D., Lee, Y. and Jung, S. “Analysis of Failure Mechanism in Anisotropic Conductive and Non-Conductive Film Interconnections”, IEEE Transactions on Components and Packaging Technologies, Vol. 31, No. 1, 2008, pp. 65-73.

[Kim08b] Kim, J., Lee, Y. and Jung, S. “Effect of Bonding Conditions on Conduction Behaviour of Anisotropic Conductive Film Interconnection”, Metals and Materials International, Vol. 14, No. 3, 2008, pp. 373-379.

[Kok10] Kokko, K. and Frisk, L. “Effects of failure criteria on the constant humidity test results”, 3rd Electronic System-Integration Technology Conference (ESTC), Berlin, Germany, September 13-16, 2010, pp. 1-4.

[Kri98] Kristiansen, H. and Liu, J. “Overview of Conductive Adhesive Interconnection Technologies for LCD's”, IEEE Transactions on Components, Packaging and Manufacturing Technology - Part A, Vol. 21, No. 2, 1998, pp. 208-214.

[Kwo04a] Kwon, W., Yang, S., Lee, S. and Paik, K. “The Effect of Tg on Thermo-mechanical Deformation and Reliability of Adhesive Flip Chip Assemblies During Temperature Cycling”, IEEE, Electronic Components

and Technology Conference, Las Vegas, USA, June 1-4, 2004, pp. 1731-1737.

[Kwo04b] Kwon, W. and Paik, K. “Contraction Stress Build-Up of Anisotropic Conductive Films (ACFs) for Flip-Chip Interconnection: Effect of Thermal and Mechanical Properties of ACFs”, Journal of Applied Polymer Science, Vol. 93, No. 6, 2004, pp. 2634-2641.

[Kwo05] Kwon, W., Yim, M., Paik, K., Ham, S. and Lee, S. “Thermal Cycling Reliability and Delamination of Anisotropic Conductive Adhesives Flip Chip on Organic Substrates With Emphasis on the Thermal Deformation”, Journal of Electronic Packaging, Vol. 127, No. 2, 2005, pp. 86-90.

[Kwo06a] Kwon, W. and Paik, K.W. “Experimental Analysis of Mechanical and Electrical Characteristics of Metal-Coated Conductive Spheres for Anisotropic Conductive Adhesives (ACAs) Interconnection”, IEEE Transactions on Components and Packaging Technologies, Vol. 29, No. 3, 2006, pp. 528-534.

[Kwo06b] Kwon, W., Ham, S. and Paik, K. “Deformation mechanism and its effect on electrical conductivity of ACF flip chip package under thermal cycling condition: An experimental study”, Microelectronics Reliability, Vol. 46, No. 2-4, 2006, pp. 589-599.

[Lah06] Lahoti, S.P., Kallolimath, S.C. and Zhou, J. “Finite Element Analysis of Thermo-hygro-mechanical Failure of a Flip Chip Package”, IEEE, 6th International Conference on Electronic Packaging Technology, Shanghai, China, August 26-29, 2006, 6p.

[Lai96] Lai, Z. and Liu, J. “Anisotropically Conductive Adhesive Flip-Chip Bonding on Rigid and Flexible Printed Circuit Substrates”, IEEE Transactions on Components, Packaging and Manufacturing Technology – Part B, Vol. 19, No. 3, 1996, pp. 644-660.

[Lau98a] Lau, J.H. “Flip Chip Technologies”, McGraw-Hill Companies Inc., United States of America, 1998, 565p.

[Lau98b] Lau, J., Wong, C.P., Prince, J.L. and Nakayama, W. “Electronic Packaging – Design, Materials, Process and Reliability”, McGraw-Hill, United States, 1998, 498p.

[Lew08] Lewis, H.J. and Coughlan, F.M. “An Overview of the Use of Electrically Conductive Adhesives (ECAs) as a Solder Replacement”, Journal of Adhesion Science and Technology, Vol. 22, No. 8-9, 2008, pp. 801-813.

[Li05] Li, Y., Moon, K. and Wong, C.P. “Electronics without Lead”, Materials Science, Vol. 308, No. 5727, 2005, pp. 1419-1420.

[Li06] Li, Y. and Wong, C.P. “Recent advances of conductive adhesives as a lead-free alternative in electronic packaging: Materials, processing,

reliability and applications", Materials Science and Engineering, Vol. 51, No. 1-3, 2006, pp. 1-35.

[Lic05] Licari, J.J. and Swanson, D.W. "Adhesives Technology for Electronic Applications – Materials, Processes, Reliability", William Andrew, Inc., Norwich, 2005, 457p.

[Lin05] Lin, Y.C. and Chen, X. "Investigation of moisture diffusion in epoxy system: Experiments and molecular dynamics simulations", Chemical Physics Letters, Vol. 412, No. 4-6, 2005, pp. 322-326.

[Lin06a] Lin, Y.C., Chen, X., Zhang, H.J. and Wang, Z.P. "Effects of hygrothermal aging on epoxy-based anisotropic conductive film", Materials Letters, Vol. 60, No. 24, 2006, pp. 2958-2963.

[Lin06b] Lin, Y.C., Chen, X. and Wang, Z.P. "Effects of hygrothermal aging on anisotropic conductive adhesive joints: experiments and theoretical analysis", Journal of Adhesion Science Technology, Vol. 20, No. 12, 2006, pp. 1383-1399.

[Lin08a] Lin, Y.C. and Chen, X. "Reliability of Anisotropic Conductive Adhesive Joints in Electronic Packaging Applications", Journal of Adhesion Science and Technology, Vol. 22, No. 14, 2008, pp. 1631-1657.

[Lin08b] Lin, Y.C. and Zhong, J. "A review of the influencing factors on anisotropic conductive adhesives joining technology in electrical applications", Journal of Material Science, Vol. 43, No. 9, 2008, pp.3072-3093.

[Liu98a] Liu, J., Lai, Z., Kristiansen, H. and Khoo, C. "Overview of Conductive Adhesive Joining Technology in Electronics Packaging Applications", IEEE, Proceedings of 3rd International Conference on Adhesive Joining and Coating Technology in Electronics Manufacturing, Binghamton, New York. September 28-30, 1998, pp. 1-18.

[Liu98b] Liu, J. "Recent advantages in conductive adhesives for direct chip attach applications", Microsystem Technologies, Vol. 5, No. 2, 1998, pp. 72-80.

[Liu99] Liu, J. "Conductive Adhesives for Electronics Packaging", Electrochemical Publications Ltd, British Isles, 1999, 432p.

[Liu02] Liu, J. and Lau, Z. "Reliability of Anisotropically Conductive Adhesive Joints on a Flip-Chip/FR-4 substrate", Journal of Electronic Packaging, Vol. 124, No. 3, 2002, pp. 240-245.

[Liu05] Liu, J., Wang, Y., Morris, J. and Kristiansen, H. "Development of ontology for the anisotropic conductive adhesive interconnect technology in electronics applications", International Symposium on Advantaged Packaging Materials: processes, Properties and Interfaces, Irvine, CA, March 16-18, 2005, pp. 193-208.

[Liu07] Liu, J., Lu, X. and Cao, L. “Reliability aspects of electronics packaging technology using anisotropic conductive adhesives”, Journal of Shanghai University, Vol. 11, No. 1, 2007, pp. 1-16.

[Liu11] Liu, J. Salmela, O. Särkkä, J. Morris, J.E. Tegehall, P. and Andersson, C. “Reliability of Microtechnology – Interconnects, Devices and Systems”, Springer, United States of America, 2011, 204p.

[Lu08] Lu, D.D. and Wong, C.P. “Recent Advantages in Developing High Performance Isotropic Conductive Adhesives”, Journal of Adhesion Science and Technology, Vol. 22, No. 8-9, 2008, pp. 835-852.

[Lu10a] Lu, D. and Wong, C.P. “Materials for Advanced Packaging”, Springer, United States of America, 2010, 719p.

[Lu10b] Lu, S. and Chen, W. “Experimental/Numerical Analysis of Thermally Induced Warpage of Ultrathin Chip-on-Flex (UTCOF) Interconnects”, IEEE Transactions on Components and Packaging Technologies, Vol. 33, No. 4, 2010, pp. 819-829.

[Luo05] Luo, S. and Wong, C.P. “Influence of Temperature and Humidity on Adhesion of Underfills for Flip Chip Packaging”, IEEE transactions on Components and Packaging Technologies, Vol. 28., No. 1, 2005, pp. 88-94.

[Lyo03] Lyons, A.M. and Dahringer, D. W. “Electrically Conductive Adhesives”, Taylor & Francis Group, LCC, in “Handbook of Adhesive Technology”, 2nd edition, edited by A. Pizzi and K.L. Mittal, Marcel Dekker, Inc., United States of America, 2003, 19p.

[Ma06] Ma, X., Jansen, K. M. B., Zhang, G. Q. and Ernst, L. J., “Hygroscopic Effects on Swelling and Viscoelasticity of Electronic Packaging Epoxy”, IEEE, 7th International Conference on Electronics Packaging Technology, Shanghai, China, August 26-29, 2006, 5p.

[Mat11] MatWeb, “Material Property Data”, available at: http://www.matweb.com (accessed 20.9.2011).

[Men08] Menard, K.P. “Dynamic Mechanical Analysis - A Practical Introduction”, 2nd edition, Taylor & Francis Group, LCC, United States of America, 2008, 224p.

[Men09] Menczel, J.D. and Prime, R.B. “Thermal Analysis of Polymers – Fundamentals and Applications”, John Wiley & Sons, Inc., New Jersey, 2009, 696p.

[Mer03] Mercado, L.L., White, J., Sarihan, V. and Lee, T.T. “Failure Mechanism Study of Anisotropic Conductive Film (ACF) Packages”, IEEE Transactions on Components and Packaging Technologies, Vol. 26, No. 3, 2003, pp. 509-516.

[Mor07] Morris, J.E. “Isotropic conductive adhesives: Future trends, possibilities, and risks”, Microelectronics Reliability, Vol. 47, No. 2-3, 2007, pp. 328-330.

[Mot96] Mottram, J.T. and Shaw, C.T. “Using Finite Elements in Mechanical Design”, McGrawn-Hill International (UK) Ltd., Great Britan, 1996, 276p.

[Mub09] Mubashar, A., Ashcroft, I.A., Critchlow, G.W. and Crocombe, A.D. “Moisture absorption-desorption effects in adhesive joints”, International Journal of Adhesion & Adhesives, Vol. 29, No. 8, 2009, pp. 751-760.

[Nat06] Nath, B., Reynolds, F. and Want, R. “RFID Technology and Applications”, IEEE, Pervasive Computing, Vol. 5, No. 1, 2006, pp. 22-24.

[Nik06] Nikitin, P.V. and Rao, K.V.S. “Theory and measurement of backscattering from RFID tags,” IEEE, Antennas and Propagation Magazine, Vol. 48, No. 6, 2006, pp. 212–218.

[Oco01] O’Conner, P. “Test Engineering – A Concise Guide to Cost-Effective Design, Development and Manufacture”, John Wiley & Sons, Ltd., England, 2001, 268p.

[Ohr98] Ohring, M. “Reliability and Failure of Electronic Materials and Devices”, Academic Press, United States of America, 1998, 692p.

[Par10] Park, J., Jang, K., Paik, K. and Lee, S. “A Study of Hygrothermal Behaviour of ACF Flip Chip Packages with Moiré Interferometry”, IEEE Transactions on Components and Packaging Technologies, Vol. 33, No. 1, 2010, pp. 215-221.

[Pro11] Professional plastics, “Mechanical Properties of Plastics”, available at: http://www.professionalplastics.com/professionalplastics/MechanicalPropertiesofPlastics.pdf (accessed 12.9.2011).

[Rao05] Rao, K.V.S., Nikitin, P.V. and Lam, S.F. “Antenna Design for UHF RFID Tags: A Review and a Practical Application”, IEEE Transactions on Antennas and Propagation, Vol. 53, No. 12, 2005, pp. 3870-3876.

[Ras04] Rasul, J.S. “Chip on paper technology utilizing anisotropically conductive adhesive for smart label applications”, Microelectronics Reliability, Vol. 44, No. 1, 2004, pp. 135-140.

[Rau06] Raugi, F., Kamruzzaman Chowdhury, M., Kristiansen, H. and Liu J. “'Flow Behaviour of Anisotropic Conductive Adhesive Film during COG Bonding Process in Flat Panel Display Assembly", ESTC, Dresden, Germany, September 5-7, 2006, pp. 827-833.

[Riz05] Rizvi, M.J., Chan, Y.C., Bailey, C., Lu, H. and Sharif, A. “The Effect of Curing on the Performance of ACF Bonded Chip-on-flex Assemblies

After Thermal Ageing", Soldering and Surface Mount Technology, Vol. 17, No. 2, 2005, pp.40-48.

[Saa08] Saarinen, K. and Heino, P. "Moisture Effects on Reliability of Non-Conductive Adhesive Attachments", Polytronic Conference, Garmish-Partenkirchen, Germany, August 17-20, 2008, 6p.

[Saa09] Saarinen, K. and Frisk, L. "Shear stress of ACA joints during temperature cycling testing", IMAPS Nordic Conference, Tønsberg, Norway, September 13-15, 2009, pp. 57-62.

[Saa10a] Saarinen, K. and Frisk, L. "Effects of Different Temperature Tests on the Reliability of ACA Joints" 34th International Microelectronics and Packaging IMAPS-CPMT Conference, Wroclaw, Poland, September 22-25, 2010, 6p.

[Saa10b] Saarinen, K., Frisk, L. and Ukkonen, L. "Moisture effects on the performance of RFID tags with ACA joints", IMAPS Nordic Conference, Göteborg, Sweden, June 6-9, 2010, 6p.

[Sep04] Seppälä, A. and Ristolainen, E. "Study of Adhesive Flip Chip Bonding Process and Failure Mechanisms of ACA joints", Microelectronics Reliability, Vol. 44, No. 4, 2004, pp. 639-648.

[Spe05] Sperling, L.H. "Introduction to Physical Polymer Science", 4th edition, John Wiley & Sons, Inc., New Jersey, 2005, 880p.

[Suh02] Suhir, E. "Accelerated Life Testing (ALT) in Microelectronics and Photonics: Its Role, Attributes, Challenges, Pitfalls, and Interaction with Qualification Tests", ASME Journal of Electronic Packaging, Vol. 124, No. 3, 2002, pp. 281-291.

[Teh04] Teh, L.K., Anto, E., Wong, C.C., Mhaisalkar, S.G., Wong, E.H., Teo, P.S. and Chen, Z. "Development and reliability of non-conductive adhesive flip-chip packages", Thin Solid Films, Vol. 462-463, 2004, pp. 446-453.

[Teh05] Teh, L.K., Teo, M., Anto, E., Wong, C.C., Mhaisalkar, S.G., Teo, P.S. and Wong, E.H. "Moisture-Induced Failures of Adhesive Flip Chip Interconnects", IEEE Transactions of Components and Packaging Technologies, Vol. 28, No. 3, 2005, pp. 506-516.

[Tsa06] Tsai, M., Wu, C., Huang, C., Cheng, W. and Yang, S. "Study of Some Parameter Effects on Warpage and Bump-Joint Stresses of COG Packages", IEEE Transactions on Advanced Packaging, Vol. 29, No. 3, 2006, pp. 587-598.

[Tsa08] Tsai, M.Y., Wu, C.Y., Huang, C.Y. and Yang, S.S. "Transient Stress Distributions in NCF-Bonded COG Packages due to Moisture Diffusion", IEEE Transactions on Advanced Packaging, Vol. 31, No. 3, 2008, pp. 454-462.

[Tum97a] Tummala, R.R., Rymanszewski, E.J. and Klopfenstein, A.G. "Microelectronics Packaging Handbook – Technology Drivers, Part I", 2nd edition, Chapman & Hall, United States of America, 1997, 720p.

[Tum97b] Tummala, R.R., Rymanszewski, E.J. and Klopfenstein, A.G. "Microelectronics Packaging Handbook - Subsystem Packaging, Part III", 2nd edition, Chapman & Hall, United States of America, 1997, 628p.

[Tum01] Tummala, R.R. "Fundamentals of Microsystems Packaging", McGraw-Hill, Inc., United States, 2001, 967p.

[Tur04] Turunen, M.P.K., Marjamäki, P., Paajanen, M., Lahtinen, J. and Kivilahti, J.K. "Pull-off test in the assessment of adhesion at printed wiring board metallisation/epoxy interface", Microelectronics Reliability, Vol. 44, No. 6, 2004, pp. 993-1007.

[Udd04] Uddin, M.A., Alam, M.O., Chan, Y.C. and Chan, H.P. "Adhesion Strength and Contact Resistance of Flip Chip on Flex Packages – Effect of Curing Degree of Anisotropic Conductive Film", Microelectronics Reliability, Vol. 44, No. 3, 2004, pp.505-514.

[Wan06] Want, R. "An Introduction to RFID Technology", IEEE Pervasive Computing, Vol. 5, No. 1, 2006, pp. 25-33.

[Wan08] Wang, W., Chan, Y.C. and Pecht, M. "Anisotropic Conductive Adhesives for Flip-Chip Interconnects", Journal of Adhesion Science and Technology, Vol. 22, No. 8-9, 2008, pp. 871-892.

[Wan09] Wang, Z., Yin, Z., Tao, B. and Xiong, Y. "Coupled Simulation of Anisotropic Conductive Adhesive Process and Reliability Analysis of the Packaging", IEEE, International Conference on Electronic Packaging Technology & High Density Packaging (ICEPT-HDP), Beijing, China, August 10-13, 2009, pp. 411-416.

[Wat04] Watabe, I., Fujinawa, T., Arifuku, M., Fujii, M. and Gotoh, Y. "Recent Advantages of Interconnection Technologies using Anisotropic Conductive Films in Flat Panel Display Applications", IEEE, 9th International Symposium on Advanced Packaging Materials: Processes, Properties and Interfaces, Atlanta, Georgia, USA, March 24-26, 2004, pp. 11-16.

[Wei02] Wei, Z., Waf, L.S., Loo, N.Y., Koon, E.M. and Huang, M. "Studies on moisture-induced failures in ACF interconnection", IEEE, Electronics Packaging Technology Conference, Singapore, December 10-12, 2002, pp. 133-138.

[Won02a] Wong, E.H., Koh, S.W., Lee, K.H. and Rajoo, R., "Comprehensive Treatment of Moisture Induced Failure - Recent Advances", IEEE, Transactions on Electronics Packaging Manufacturing, Vol. 25, No. 3, 2002, pp. 223-230.

[Won02b] Wong, E.H., Koh, S.W., Lee, K.H. and Rajoo, R. “Advanced Moisture Modeling & Characterisation for Electronic Packaging”, IEEE, Electronic Components and Technology Conference, San Diego, California, USA, 2002, pp. 1297-1303.

[Wun08] Wunderle, B., Kallmayer, C., Walter, H., Braun, T., Michel, B. and Reichl, H. “Lifetime Model for Flip-Chip on Flex Using Anisotropic Conductive Adhesive under Moisture and Temperature Loading”, IEEE, 11th Intersociety Conference on Thermal and Thermomechanical Phenomena in Electronic Systems (ITHERM), Orlando, FL, USA, May 28-31, 2008, pp. 799-808.

[Wun09] Wunderle, B., Kallmayer, C., Walter, H., Braun, T., Gollhardt, A., Michel, B. and Reichl, H. “Failure modelling of ACA-glued flip-chip on flex assemblies”, Microsystem Technologies, Vol. 15, No. 1, 2009, pp. 3-15.

[Yeo04] Yeo, A., Teo, M. and Lee, C. “Thermo- and Hydro-mechanical Modeling of an Adhesive Flip Chip Joint”, IEEE, Electronics Packaging Technology Conference, Singapore, December 8-10, 2004, pp. 92-97.

[Yeu98] Yeung, N.H., Wu, C.M.L. and Lai, J.K.L. “Thermal Cycling Analysis of TAB OLB Connection With ACF”. Proceedings of the 3rd International Conference on Adhesive Joining and Coating Technology in Electronics Manufacturing, Binghamton, New York, September 28-30, 1998, pp. 206-210.

[Yim98] Yim, M. and Paik, K. “Design and Understanding of Anisotropic Conductive Films (ACF’s) for LCD Packaging”, IEEE Transactions on Components, Packaging, and Manufacturing Technology – Part A, Vol. 21, No. 2, 1998, pp. 226-234.

[Yim99] Yim, M. and Paik, K. “The Contact Resistance and Reliability of Anisotropically Conductive Film (ACF)”, IEEE Transactions on Advanced Packaging, Vol. 22, No. 2, 1999, pp. 166-173.

[Yim03] Yim, M., Hwang, J., Kwon, W., Jang, K.W. and Paik, K. “Highly Reliable Non-Conductive Adhesives for Flip Chip CSP Applications”, IEEE Transactions on Electronics Packaging Manufacturing, Vol. 26, No. 2, 2003, pp. 150-155.

[Yim06] Yim, M.J. and Paik, K.W. “Recent advantages on anisotropic conductive adhesives (ACAs) for flat panel displays and semiconductor packaging applications”, International Journal of Adhesion & Adhesives, Vol. 26, No. 5, 2006, pp. 304-313.

[Yim07] Yim, M.J., Hwang, J. and Paik, K.W. “Anisotropic conductive films (ACFs) for ultra-fine pitch Chip-on-Glass (COG) applications”, International Journal of Adhesion & Adhesives, Vol. 27, No. 1, 2007, pp. 77-84.

[Yim08] Yim, M.J., Li, Y., Moon, K., Paik, K.W. and Wong, C.P. “Review of Recent Advantages in Electrically Conductive Adhesive Materials and Technologies in Electronic Packaging”, Journal of Adhesion Science and Technology, Vol. 22, No. 14, 2008, pp. 1593-1630.

[Yin03] Yin, C.Y., Lu, H., Bailey, C. and Chan, Y.C. “Experimental and Modelling Analysis of the Reliability of the Anisotropic Conductive Films”, IEEE, Electronic Components and Technology Conference, New Orleans, Louisiana, USA, May 27-30, 2003, pp. 698-702.

[Yin05a] Yin, C.Y., Lu, H. Bailey, C. and Chan, Y.C. “Moisture Effects on the Reliability of Anisotropic Conductive Films”, IEEE, 6th International Conference on Thermal, Mechanical and Multiphysics Simulation and Experiments in Micro-Electronics and Micro-Systems, EuroSimE, Berlin, Germany, April 18-20, 2005, pp. 162-167.

[Yin05b] Yin, C.Y., Lu, H. Bailey, C. and Chan, Y.C. “Experimental and Modelling Analysis on Moisture Induced Failures in Flip Chip on Flex Interconnections with Anisotropic Conductive Film”, IEEE, International Conference on Asian Green Electronics, Shanghai, China, March 15-18, 2005, pp. 172-177.

[Yin06] Yin, C.Y., Lu, H. Bailey, C. and Chan, Y.C. “Macro-micro modelling of moisture induced stresses in an ACF flip chip assembly”, Soldering & Surface Mount Technology, Vol. 18, No. 2, 2006, pp. 27-32.

[Yoo09] Yoon, J., Kim, I. and Lee, S. “Measurement and Characterization of the Moisture-Induced Properties of ACF Package”, Journal of Electronic Packaging, Vol. 131, No. 2, 2009, 8p.

[Yu04] Yu, H., Mhaisalkar, S.G., Wong, E.H. and Caers, J.F.J.M. “Evolution of Mechanical Properties and Cure Stresses in Non-Conductive Adhesives Used for Flip Chip Interconnects”, IEEE, Electronics Packaging Technology Conference, Singapore, December 8-10, 2004, pp. 468-472.

[Zho05a] Zhong, Z.W. “Various Adhesives for Flip Chips” Journal of Electronic Packaging, Vol. 127, No. 1, 2005, pp. 29-32.

[Zho05b] Zhou, J., Tee, T.Y., Zhang, X. and Luan, J. “Characterization and Modeling of Hygroscopic Swelling and its Impact on Failures of a Flip Chip Package with No-flow Underfill”, IEEE, Electronics Packaging Technology Conference, Singapore, December 7-9, 2005, pp. 561-568.

[Zho05c] Zhou, J., Lahoti, S.P., Sitlani, M.P., Kallolimath, S.C. and Putta, R. “Investigation of Non-Uniform Moisture Distribution on Determination of Hygroscopic Swelling Coeffecient and Finite Element Modeling for a Flip Chip Package”, IEEE, 6th International Conference on Thermal, Mechanical and Multiphysics Simulation and Experiments in Micro-Electronics and Micro-Systems, EuroSimE, Berlin, Germany, April 18-20, 2005, pp.112-119.

[Zie94] Zienkiewicz, O.C. and Taylor, R.L. “The Finite Element Method – Volume 1 – Basic Formulation and Linear Problems”, 4th edition, McGrawn-Hill International (UK) Limited, UK, 1994, 648p.

Tampereen teknillinen yliopisto
PL 527
33101 Tampere

Tampere University of Technology
P.O.B. 527
FI-33101 Tampere, Finland

ISBN 978-952-15-2759-3
ISSN 1459-2045